Ligand recombination and a hierarchy of solvent slaved dynamics: The origin of kinetic phases in hemeproteins

ARTICLE *in* GENE · SEPTEMBER 2007

Impact Factor: 2.14 · DOI: 10.1016/j.gene.2007.04.032 · Source: PubMed

4 AUTHORS, INCLUDING:

Uri Samuni
City University of New York - Queens College
43 PUBLICATIONS **1,490** CITATIONS

SEE PROFILE

Camille Roche
Albert Einstein College of Medicine
39 PUBLICATIONS **507** CITATIONS

SEE PROFILE

Joel M Friedman
Albert Einstein College of Medicine
255 PUBLICATIONS **8,496** CITATIONS

SEE PROFILE

Published in final edited form as:
Gene. 2007 August 15; 398(1-2): 234–248.

Ligand recombination and a hierarchy of solvent slaved dynamics: the origin of kinetic phases in hemeproteins

Uri Samuni, **David Dantsker**, **Camille Roche**, and **Joel M. Friedman***
Albert Einstein College of Medicine, Department of Physiology and Biophysics, Bronx, New York 10461, USA

Abstract

Ligand recombination studies play a central role both for characterizing different hemeproteins and there conformational states but also for probing fundamental biophysical processes. Consequently, there is great importance to providing a foundation from which one can understand the physical processes that give rise to and modulate the large range of kinetic patterns associated with ligand recombination in myoglobins and hemoglobins. In this work, an overview of cryogenic and solution phase recombination phenomena for COMb is first reviewed and then a new paradigm is presented for analyzing the temperature and viscosity dependent features of kinetic traces in terms of multiple phases that reflect which tier(s) of solvent-slaved protein dynamics is(are) operative on the photoproduct population during the time course of the measurement. This approach allows for facile inclusion of both ligand diffusion among accessible cavities and conformational relaxation effects. The concepts are illustrated using kinetic traces and MEM populations derived from the CO recombination process for wild type and mutant myoglobins either in sol-gel matrices bathed in glycerol or in trehalose derived glassy matrices.

Keywords

myoglobin; carbonmonoxide; sol-gel; trehalose; geminate recombination; Xe cavities

1. Ligand recombination

Studies utilizing ligand recombination subsequent to photodissociation continue to provide basic insight into the functional properties of the many varieties of hemoglobin and myoglobin like molecules that are found through out the animal and plant worlds. Such studies are significant for several reasons all of which stem from the sensitivity of the recombination process to global structure, site specific effects and dynamics. Ligand recombination data at ambient temperatures are often useful in establishing potential functions of a newly described hemeproteins as well as routinely being used in exploring structure-function correlations in well characterized molecules such as human hemoglobin and mammalian myoglobins. Ligand recombination in myoglobin in particular has provided biophysics with a process that has allowed for dramatic advances in understanding: i) protein dynamics, ii) the role of protein dynamics in modulating protein reactivity and iii) the interplay between the dynamical properties of the protein and the surrounding solvent. Despite the heavy focus on understanding

*corresponding author: Address: Albert Einstein College of Medicine, Department of Physiology and Biophysics, Bronx, New York 10461, USA, Tel. 718 430 3591, Fax 718 430 8819, Email jfriedma@aecom.yu.edu.

the biophysical determinants of ligand recombination in hemeproteins, a unified molecular level model that accounts for the features of ligand recombination under a wide variety of experimental conditions is still lacking. In the present work, we present: i) an overview of earlier descriptions and models, ii) a new integrated framework that can readily account for the role of conformation, residue composition, dynamics and solvent dependence and iii) examples of CO recombination in wild type and mutant sperm whale myoglobin that illustrate the elements of the new framework.

A major objective in the presented work is to provide a framework that links the many kinetic studies of myoglobin at both cryogenic and ambient temperatures. The cryogenic studies have to a large degree focused on using ligand recombination as a tool with which to probe protein dynamics and ligand migration within the protein matrix. Typically, ambient temperature studies neither address the role of protein dynamics nor get utilized to expose the organizational makeup of dynamical processes in proteins. The present treatment represents a distillation and out growth of our recent work utilizing sol-gel encapsulation and glassy matrices to modulate protein dynamics in a way that provides a direct bridge between cryogenic and ambient domains (Dantsker et al., 2002; Dantsker et al., 2005a; Dantsker et al., 2005b). We (Khan et al., 2000; Dantsker et al., 2002; Samuni et al., 2002; Dantsker et al., 2005a; Dantsker et al., 2005b) and others (Sottini et al., 2004; Sottini et al., 2005a; Sottini et al., 2005b; Sottini et al., 2005c) have shown that this approach of using high viscosity solvents and matrices exposes the dynamical events that give rise to the solution phase functional properties observed in solution at ambient temperatures.

2. Protein dynamics

Understanding how proteins function on a detailed molecular level is a major objective in biophysics. Characterizing equilibrium structures of proteins does not always provide an adequate molecular level explanation for the observed reactivity even for many of the most extensively studied systems. The influence of protein dynamics is often the key element missing in developing a comprehensive explanation of protein function. A major challenge in understanding the functional role of protein dynamics arises from there being many types of motions associated with proteins whose influence on function can be both time domain dependent and solvent dependent. Hence the need for organizing dynamics into a hierarchical scheme that reflects both the time domain under which they are operative and the responsiveness of the different groupings to solvent properties such as viscosity. The approach taken in the present work builds on the work of Frauenfelder and coworkers (Frauenfelder et al., 2002; Frauenfelder et al., 2006), who have promoted the idea of organizing dynamics into a hierarchy based on the degree to which the dynamics are slaved (i.e. coupled) to motions of the surrounding solvent or matrix.

3. Mb: kinetics and dynamics

It is apparent that proteins are inherently complex materials (Frauenfelder et al., 1991; Frauenfelder, 1995; Frauenfelder et al., 2001). Even the simplest protein reactions often exhibit layers of complexity that were not anticipated a few decades ago. A case in point is the heavily studied process by which photodissociated carbon monoxide rebinds to the heme in myoglobin (Mb) (Antonini and Brunori, 1971). This specific reaction, on a continuing basis, persists in yielding new insights into fundamental protein biophysics.

Much of the work on Mb has been directed at exposing the biophysical principles responsible for the observed kinetic patterns associated with ligand binding or rebinding. In aqueous solution at ambient temperatures, the rebinding of CO to photodissociated COMb occurs in two phases. The faster phase (extending from picoseconds to microseconds) is geminate recombination arising from CO concentration-independent rebinding from within the protein

(Alpert et al., 1979; Duddell et al., 1979; Friedman and Lyons, 1980; Henry et al., 1983). The second phase, designated as S→A, is a CO-concentration dependent rebinding attribute to the rebinding of solvent-equilibrated CO (Antonini and Brunori, 1971). For wild-type Mb (horse or sperm whale), the yield of geminate recombination in solution is only a few percent, reflecting a high probability that the photodissociated CO equilibrates with the solvent prior to rebinding.

4. Recombination studies in solution

Kinetic studies on Mb mutants in solution at ambient temperatures by Olson (Quillin et al., 1995; Olson and Phillips, 1996; Scott et al., 2000; Draghi et al., 2002) indicate that ligand entry from the solvent into the protein is via the E7 distal gate, which transiently opens due to thermally mediated fluctuations. It was also concluded from these studies that the ligand escape process also occurs via the distal gate. Recombination studies in which the Mb was exposed to Xe gas at high pressure (Scott and Gibson, 1997) revealed that the geminate phase was comprised of two phases: one in which the rebinding was directly from the distal heme pocket and the other where the rebinding was from a much larger accessible volume that could be blocked in the presence of Xe gas. That results was explained in terms of the dissociated ligand accessing well-defined packing defect sites within the protein that have become known as Xe cavities (Schoenborn et al., 1965; Tilton et al., 1984). The Xe gas studies as well as recombination studies on mutants that have the Xe cavities blocked (Scott et al., 2001; Draghi et al., 2002), revealed a pattern that is consistent with a proposed model by Olson and coworkers (Scott et al., 2001) in which ligand entry and escape from Mb is via the distal heme pocket and the Xe cavities function as a “baseball glove”-like entropic sink (through volume enhancement) that allows for trapping of the incoming ligand.

5. Recombination studies at cryogenic temperatures

Recombination studies at cryogenic temperatures (< 60° K), revealed a kinetic pattern indicative of there being a frozen distribution of functionally distinct conformational substates (cs) (Austin et al., 1973; Austin et al., 1975). Under these conditions CO rebinding occurs through a single phase (also referred to as Process I), containing contributions from the frozen distribution of functionally distinct conformational substates (Austin et al., 1973; Austin et al., 1975). Each substate undergoes recombination with a distinct rate thereby giving the overall recombination process kinetic features characterized by a fixed distribution of different recombination rates. Under these conditions, kinetic hole burning (KHB) phenomena can be observed (Campbell et al., 1987; Agmon, 1988; Srajer and Champion, 1991; Steinbach et al., 1991), due to the mapping of the frozen distribution of kinetic barriers onto inhomogeneously broadened spectroscopic line shapes.

With increasing temperature, a progression of dynamics-associated phenomena is observed. There is a loss of kinetic hole burning effects, and the onset of dynamic hole filling, attributed to thermal activation of conformational fluctuations that mediate conformational averaging of the functionally distinct conformational substates (Huang et al., 1997). Most obvious is the progressive onset of new kinetic phases occurring with increasing temperature (Austin et al., 1973; Austin et al., 1975; Steinbach et al., 1991; Doster et al., 1993; Agmon et al., 1994; Kleinert et al., 1998). The onset of new rebinding phases is attributed to the thermal activation of dynamics that mediate the onset of processes that slow the faster kinetic phase observed at the lower temperatures (Process I). The net effect is that the overall recombination kinetics exhibit an inverse temperature effect i.e. the overall kinetics slow with increasing temperature. The kinetic barrier for rebinding is observed to undergo a substantial increase in going from the cryogenic limit to the aqueous solvent limit. It has also been shown that a significant component of the inverse temperature effect is due to changes in the recombination process

resulting from the temperature-dependence of the solvent viscosity (Ansari et al., 1992; Hagen et al., 1996). To an extent, the inverse temperature effect is an inverse viscosity effect in which the overall recombination process gets slower with decreasing viscocity

The origin of both the onset of the new phases and the related inverse temperature/viscosity effect has been vigorously explored and debated. The central focus was whether these processes were being driven by barrier-raising conformational relaxations (Agmon and Hopfield, 1983; Ahmed et al., 1991; Ansari et al., 1992; Abadan et al., 1995) or by increased access of the dissociated ligand to slow rebinding docking sites (Powers et al., 1987; Srajer et al., 1991) within the protein matrix by the dissociated CO. Initially, the spectroscopic and theoretical work favored the barrier raising relaxation model. Subsequently, the unambiguous demonstration that dissociated CO could access packing defect (Xe cavities) within the protein (Schoenborn et al., 1965; Tilton et al., 1984) provided compelling support for the slow rebinding docking site models (Hartmann et al., 1996; Scott and Gibson, 1997; Brunori et al., 1999; Brunori et al., 2000; Ostermann et al., 2000; Scott et al., 2000; Srajer et al., 2001; Bourgeois et al., 2003; Kriegl et al., 2003; Nienhaus et al., 2003b; Nienhaus et al., 2003a; Schotte et al., 2003; Lamb et al., 2004; Tetreau et al., 2004); however, these results do not preclude a significant role for a barrier increase via conformational relaxation.

6. Nomenclature for Mb states and processes

Nomenclature has been evolving both for spectroscopically and kinetically distinct states of Mb and for the various kinetic phases. The evolution stems both from the two distinct approaches to the inverse temperature effect and from the different techniques, solvent conditions and time resolutions used for probing conformations and kinetic pathways. Two extremes are encountered. In one case the cryogenic-based nomenclature refers to the location of the ligand. Initially there were the A, B, C and S states referring to respectively: i) the ligand being bound to heme-iron, ii) unbound but localized in the distal heme pocket (DHP), iii) localized in the protein matrix and iv) localized in the solvent. Rebinding from the DHP was referred to as either Process I or B→A. Rebinding after the ligand had migrated from the DHP to the “bulk matrix” of the protein was referred to either as the matrix process or C→A; whereas, the solvent phase was used to describe S→A. With the discovery of the Xe cavity docking sites and the spectroscopic/crystallographic identification at cryogenic temperatures of a distinct progression of ligand localization sites in the matrix, the nomenclature was expanded to include a D state. Now the state C referred to the ligand being in the closer Xe4 cavity and the D state to localization in the more distant Xe1 cavity on the proximal side of the heme.

The relaxation-oriented second approach for the nomenclature gave rise to the Mb and Mb* designations referring respectively to rebinding associated with: i) the fully relaxed equilibrium conformation of the unliganded species and ii) the unrelaxed conformation associated with the initial liganded species. Recent findings have exposed the limitations of both approaches (Bourgeois et al., 2003; Schotte et al., 2003; Hummer et al., 2004; Lim et al., 2004; Schotte et al., 2004; Lim and Anfinrud, 2005; Aranda et al., 2006; Bourgeois et al., 2006) (Dantsker et al., 2002; Dantsker et al., 2005a; Dantsker et al., 2005b). Clearly, both ligand migration and conformational relaxation contribute to the overall kinetic patterns. Most significant is that at all but the lowest temperatures, ligand equilibration among the different Xe cavities subsequent to migration from the DHP is likely to be faster than “matrix rebinding processes” making it impossible to attribute a given kinetic phase to rebinding from a specific Xe cavity. In the following section, we describe our attempt at a new framework that builds on the earlier nomenclature and incorporates the new insights.

7. The new formalism

Recent CO recombination studies on Mb mutant encapsulated in porous sol-gel matrices and trehalose-derived glasses (Dantsker et al., 2002; Dantsker et al., 2005a; Dantsker et al., 2005b), have been leading us to a composite model to account for the role of both dynamics and accessible volume in modulating ligand rebinding kinetics in Mb. The model is also based on the following concepts pertaining to the nature of protein dynamics:

1. Protein dynamics can be organized hierarchically based on the degree to which they are slaved to the motions of the surrounding solvent (Fenimore et al., 2002; Frauenfelder et al., 2002; Lubchenko et al., 2005; Frauenfelder et al., 2006).
2. The degree to which a given tier of dynamics is slaved to the solvent defines a time scale over which those dynamics are not operative with respect to impacting protein properties. For example, femtosecond probing of a protein ensemble does not reveal fluctuations or relaxations occurring on the picosecond or slower time scales. In contrast, a measurement made over a nanosecond window reflects the impact of dynamics operating of the picosecond time scale but not the millisecond time scale.
3. The hierarchy of dynamics based on slaving thus also gives rise to an ordering of dynamics based on the temporal onset of influence on protein properties.
4. For a given solvent and given temporal window over which the protein properties are being probed, only those dynamics that are operative during that window will contribute to the observed phenomena.
5. The onset of influence of the most strongly slaved tiers of dynamics will undergo the largest degree of slow down with progressive increase in the local viscosity of the surrounding solvent (Fenimore et al., 2002; Frauenfelder et al., 2002; Lubchenko et al., 2005; Frauenfelder et al., 2006). As a consequence, high viscosity conditions will allow for increased ease with which the impact of different tiers of dynamics can be differentiated.
6. There is a progression of time windows starting at some observation point time t, that represent the successive onset of influence of progressively more slaved tiers of dynamics. Hence, if at time zero there is a rapidly initiated process that can be followed over an extended time period; then, there will be an initial period where the influence of most of the solvent slaved tiers of dynamics are not reflected in an initial observation window. Eventually different tiers of dynamics start to exert influence. The onset of influence from the most strongly slaved dynamics will occur after the longest time window (referenced from time zero) whereas the less slaved dynamics exert impact after shorter windows.

Ligand recombination in hemeproteins is an ideal molecular-level laboratory for the study of these effects due to both the use of the dissociation event as a time marker for time zero and the extensive time window over which the recombination process occurs. The long “probe” window connected with the recombination provides a time line over which signatures for the successive onset of the different tiers of dynamics can be observed.

For the recombination of CO to Mb, we define four states designated as A, B, C and D. The A state refers to the state in which the CO is bound to the heme and the other three states all have the CO dissociated from the heme-iron but are differentiated based on which tiers of dynamics are influencing the recombination. Since both ligand migration and conformational relaxation can occur within the same time window, the state designations, with the exception the A state, do not refer specifically to either the localization site of the ligand or the specific relaxation occurring. Instead they refer to which tier(s) of dynamics is (are) operative during

the lifetime of the state. The B, C and D states are each associated with distinct recombination phases that reflect the impact of the different tiers of dynamics.

Two distinct tiers of relevant dynamics have been identified based on the degree to which they are slaved to the motions of the surrounding solvent and the temporal window before which they start to exert influence on the observable phenomena (Dantsker et al., 2005a; Dantsker et al., 2005b). These two tiers of dynamics are comprised of dynamics that we refer to as C and D state dynamics. The C state dynamics are less solvent slaved than the D state dynamics. Under enhanced viscosity conditions the C state dynamics will become operative on shorter time scales (short onset window) relative to the more highly solvent slaved D state dynamics (long onset window). The tier of C state dynamics consists of various side chain fluctuations and small scale side chain relaxations. These side chain fluctuations facilitate ligand diffusion within the protein and can increase the barrier for rebinding due to partial relaxation of distal residue side chains. The second tier, comprised of the D state dynamics, which begins to manifest influence after a longer time delay subsequent to time zero, is comprised of larger amplitude dynamics. The D state dynamics include the volume changing protein fluctuations that allow the entry and escape of small molecules (water, ligands) into and out of the protein via the distal (heme) pocket gate. In earlier work, it was directly shown that for a given high viscosity solvent/matrix, the C and D state tiers manifested low and high activation energies respectively (Dantsker et al., 2005b). In this earlier work the C and D state tiers were designated as pre-HAM (heme access modes) and HAM dynamics respectively. Based both on a larger series of measurements (to be published) of the activation energies associated with the onset of the influence of the C and D state dynamics and a more limited set of measurements on Mbs (Frauenfelder et al., 2002; Frauenfelder et al., 2006), we tentatively assign the C state and D state dynamics to tiers that are slaved to the β and α fluctuations of the hydration shell and bulk solvent layers respectively. Under high viscosity conditions the β and α fluctuations can be distinguished based on temperature dependence. The former refers to the librational motions of the molecules comprising the hydration shell whereas the latter refer to the larger translational motions of the molecules in the bulk solvent. The α fluctuations are fully damped below the glass transition of the solvent whereas the β fluctuations persist at temperatures well below the glass transition.

For the photodissociated population of Mb molecules, we now define the B state as the “state” of the dissociated system that exists from the time period starting from the instant of photodissociation and extending for the temporal window over which neither the C or the D state dynamics are operative. The term state is loosely used in these definitions for lack of a better term. The B, C and D state really refer to time windows defined based on which dynamics are operative. With the onset of the influence of the C state tier of dynamics, the B state decays into the C state. Similarly, the C state gives way to the D state when the D state dynamics begin to impact the behavior of the system. The recombination phases occurring during the lifetime of the B, C and D states are designated as B→A, C→A and D→A respectively. When all three kinetic phases are observed in the same kinetic trace (vide infra), the temporal termination points of the B→A and C→A recombination phases represent the onset of influence of the C state and D state dynamics, respectively. Thus the onset of influence for each of these two tiers is reflected in temporal signatures in the overall kinetic traces for the CO recombination.

This approach to protein states and dynamics is general in that for any given time dependent measurement, one can describe the B(window), C(window) and D(window) states that reflect which tier(s) of dynamics are operating on the system during that measurement.

This formalism provides a direct link to the earlier cryogenic and solvent phase studies in that the different tiers of dynamics are responsible for the relaxations and ligand migrations that are observed in these studies. The B(window) state refers to the time window starting from the

instant of dissociation and persisting to the onset of the influence of the C state tier of dynamics. Within the B state time window, the dissociated ligand is typically localized within the distal heme pocket (DHP) but is not experiencing the influence of either the C or D state dynamics. Under these conditions the recombination kinetics (Process I) are distributed (Austin et al., 1973; Austin et al., 1975) and kinetic hole burning (KHB) (Campbell et al., 1987; Agmon, 1988; Chavez et al., 1990; Srajer and Champion, 1991; Steinbach et al., 1991; Nienhaus et al., 1992) is observed both phenomena due to the frozen distribution of functionally distinct conformational substates. Thermal activation of conformational averaging that terminates the KHB effect is seen in dynamic hole filling phenomena (Huang et al., 1997) observed at cryogenic temperatures. The temperature dependence of the hole filling is suggestive of C state dynamics driving that process.

The C (window) state begins with the onset of the influence of the C state tier of dynamics and persists until the onset of the influence of the D state tier of dynamics. Under the influence of the C state tier of dynamics the dissociated ligand is not necessarily localized within the DHP but can instead diffuse through the full accessible volume of the protein (Xe cavities plus the DHP) powered by low amplitude side chain fluctuations that belong to the C state tier of dynamics. Localization within the distal hemepocket does not necessarily imply a B state since large side chains blocking escape from the distal hemepocket (e.g. tryptophan at position E11) can limit facilitated diffusion into the Xe cavities even after the onset of the C state dynamics. The D (window) state refers to the protein plus dissociated ligand during the temporal window when both tiers of dynamics are operative on the protein. Thus the dissociated ligand is subject to residue side chain facilitated diffusion throughout the full accessible volume of the protein but with the additional influence of the large amplitude dynamics within the D state tier. The large amplitude fluctuations of the D state tier allow for ligand escape as well as for potential entry of water into the transiently vacated distal heme pocket. Thus in the case of photodissociated COMb, the B, C and D states represent the photoproduct protein plus dissociated ligand experiencing progressive changes in functional properties based on a progression of time windows that are defined by the viscosity/temperature dependent onset of the influence of different tiers of dynamics.

A visual summary of this new designation of states/windows is shown in Fig. 1. The pale blue ovals filling the Xe cavities for the B state signify that these cavities are not accessible during the temporal window that delineates the lifetime of the B state. The internal and external double headed black arrows represent the C and D state dynamics respectively. The colored ball shown external to the left side of the D state protein with the two headed arrow linking it to the entrance of the distal heme pocket (DHP) represents the D state dynamics-mediated entering and exiting of either ligands or solvent molecules.

8. Overview of recombination phases and the dynamics that modulate them

8.1. B→A

The B→A recombination phase refers to rebinding of the photodissociated ligand typically localized within the distal heme pocket (DHP) prior to the onset of the influence of C state tier of dynamics which are responsible for the side chain facilitated diffusion of the ligand from the DHP into the adjacent Xe cavities. This phase is what is typically observed (Austin et al., 1973; Austin et al., 1975)for recombination at very low cryogenic temperature conditions (< 100 K). Two kinetic sub-phases have been identified (Tetreau et al., 2004; Dantsker et al., 2005a; Dantsker et al., 2005b)which have been referred to as: B→A and B′→A. These two phases are attributed to rebinding from sites within the distal heme pocket that are close to the heme-iron and removed from the heme-iron respectively. Such sites have been directly observed both in time resolved crystallographic (Bourgeois et al., 2003; Schotte et al., 2003;

Wullf et al., 2003; Lim et al., 2004; Schotte et al., 2004) as well as in simulation studies (Teeter, 2004).

8.2. C state dynamics

The umbrella designation of C state dynamics, include the side chain fluctuations and small amplitude relaxations that initiate and modulate the C→A recombination phases. The C→A phase is the first major set of recombination phases occurring subsequent to the B→A recombination. The C state dynamics are thermally activated but with low activation energies (Dantsker et al., 2005b) that are consistent with slaving to the β fluctuations of the hydration shell. They occur even in glassy matrices (Cordone et al., 1998; Librizzi et al., 2002; Abbruzzetti et al., 2005; Cordone et al., 2005; Dantsker et al., 2005a; Dantsker et al., 2005b) as long as the matrix is not totally rigidified as in the case of extremely dry glasses where only the B→A recombination phase is observed for COMb even at ambient temperatures (Cordone et al., 2005). The C state dynamics appear to be associated primarily with side chain fluctuations that serve to: i) facilitate diffusion of the dissociated ligand both out of the distal hemepocket into the Xe cavities and between the accessible cavities of the protein, ii) transiently open connections between intra-protein cavities and iii) slightly enhance the enthalpic barrier for recombination through partial relaxation of side chains to positions that hinder access of the dissociated ligand to the heme iron. The hindered access decreases the probability of ligand rebinding when the dissociated ligand reenters the DHP as it explores via the facilitated diffusion, the accessible volume of Mb. Thus the C state dynamics create the slower family of C→A recombination phases by entropically stabilizing the C state relative to the B state by virtue of increased accessible volume for the dissociated ligand and by increasing the barrier for accessing the heme-iron by the dissociated ligand.

Specific dynamical processes that comprise the C state tier can be separated based on moderate differences in activation energy and onset of influence time points. Each set of dynamics having a successively slower onset point creates a new substate (window) within the C manifold (e.g. C, C′, C″..) and a corresponding progressive slow down (lengthening) of the overall C→A recombination phase. As a consequence, these distinct members of the sub-tier of C state dynamics (C, C′, C″.state dynamics) give rise to progressively slower recombination phases (C, C′, C″… → A) that can give that overall recombination phase a highly nonexponential appearance if the C, C′, C″… states are sufficiently well-separated in time and are sufficiently different with respect to properties that slow down the recombination kinetics.

8.3. C→A

C→A refers to the rebinding phase (s) occurring within the C state and therefore manifest the influence of the C state tier of dynamics. The C→A family of recombination phases was initially referred to as the matrix process in the early cryogenic studies (Austin et al., 1973; Doster et al., 1993). As noted above the slow down of this family of kinetic phases relative to the B→A kinetic phases is due to both the increased accessible volume which entropically stabilizes the C states over the B states and the increased enthalpic barrier for recombination due to hindered access to the heme-iron.

8.4. D state dynamics

The D state dynamics that are responsible for the C→D state transition, the termination of the C→A recombination phase and the appearance of the D→A recombination phase appear to be associated with large volume changing conformational fluctuations that allow for ligand entry from the solvent into Mb and ligand escape from Mb to the solvent via the so called “distal gate”. The recombination phases that temporally precede the D→A phase are occurring under the modulating influence of those dynamics that do not require large global volume changing fluctuations. The large amplitude dynamics of the D state are readily damped in rigid media

(Cordone et al., 1998; Dantsker et al., 2002; Librizzi et al., 2002; Abbruzzetti et al., 2005; Cordone et al., 2005; Dantsker et al., 2005a; Dantsker et al., 2005b). In glassy matrices they become manifest near or at the glass transition temperature of the surrounding solvent (Dantsker et al., 2002; Dantsker et al., 2005a; Dantsker et al., 2005b). We have recently observed that for ligand-free Mb and Hb derivatives embedded in either NO or CO perfused dry trehalose-derived glasses, the appearance of liganded derivatives does not occur until the glass is heated to near the glass transition temperature. Similarly, the appearance of spectroscopic evidence of water accessing the distal heme pocket also does not become apparent until at or near the glass transition temperature of the trehalose glass.

8.5. D→A

D→A refers to rebinding occurring within the D state. Thus for the D→A recombination, the ligand is diffusing among the Xe cavities as in the C state but the barrier for recombination has increased due to the relaxations associated with the D state tier of dynamics. The substantial slow down in the recombination kinetics for the D→ A phase relative to the faster C→ A family is due to both the larger amplitude conformational relaxations (vis a vis those of the C state tier of dynamics) that further enhance the enthalpic barrier for ligand-heme bond formation and the entry of water into the DHP which both hinders access to the heme and increases the probability for ligand escape from the DHP. For CO, this slow phase is often indistinguishable from what is often referred to as the S→A or solvent phase (also referred to as the bimolecular phase) recombination. This situation would occur when ligand entry into the protein is not rate limiting (high relative concentration of CO to protein) and the recombination kinetics are governed by the binding of a ligand that is freely accessing the Xe cavities and DHP under conditions where the heme environment is fully relaxed to that of the stable or quasi-stable deoxy derivative under the given solvent conditions (vide infra). Since, ligand entry into Mb requires the large amplitude D state dynamics and since ligand capture requires accessing the extended volume (DHP and Xe4), any CO that has accessed the Xe cavities from either the solvent or from a dissociation process within the DHP will be subject to the same dynamical influences.

8.6. Other tiers of dynamics and their impact on recombination

The above description does not cover the influence of other tiers of dynamics that occur on an even slower time scale than those of the D state tier. These would include for Mb, the dynamics contributing to the relaxation of the initial photoproduct tertiary structure back to the equilibrium deoxy conformation and for hemoglobins the additional larger scale motions required for changes in quaternary structure. Both categories of dynamics can be greatly slowed within sol-gel matrices relative to the operative time scales of the C and D tiers of dynamics (Bettati and Mozarrelli, 1997; Das et al., 1999; Khan et al., 2000; Abbruzzetti et al., 2001; Dantsker et al., 2002; Samuni et al., 2002; Shibayama and Saigo, 2003; Samuni et al., 2004; Viappiani et al., 2004). Consequently, the above A, B, C and D scheme can be explored within the conformational boundaries of different trapped tertiary and quaternary structures that represent both equilibrium and nonequilibrium conformational distributions. Thus we can designate the A, B, C or D state for any tertiary/quaternary state that persist on a time scale that is much longer than the recombination process. For hemoglobins encapsulated within sol-gel matrices, these four states can be used to describe the recombination within the low and high affinity members of the T state family of structures (Bruno et al., 2001; Dantsker et al., 2004; Samuni et al., 2004; Viappiani et al., 2004; Samuni et al., 2006) as well as the deoxy R and liganded R conformations. The current description can also be expanded include the very weakly slaved low energy activation dynamics that drive the conformational averaging that causes dynamic hole filling as well as possible movement of the ligand within the distal hemepocket during the B state window.

9. Examples illustrating the new formalism

The following section will show how the recombination traces from several different Mbs under high viscosity conditions can be readily analyzed and understood based on the A, B, C and D state model described above. The kinetic data are largely derived from our earlier work (Dantsker et al., 2002; Dantsker et al., 2005a; Dantsker et al., 2005b) but the kinetic traces and the maximum entropy method (MEM) derived kinetic populations are configured to illustrate the concepts associated with the new model. The data is derived from two types of samples: sol-gel encapsulated COMb bathed in glycerol and COMb embedded in trehalose derived glassy matrices. The preparative protocols and the techniques for generating the CO recombination traces are described in earlier works (Dantsker et al., 2002; Dantsker et al., 2005a; Dantsker et al., 2005b). MEM analysis of the recombination traces is used as previously described (Dantsker et al., 2005a; Samuni et al., 2006) to expose the distinct kinetic populations that contribute to the overall kinetics. The samples used in this study, (provided by John Olson) are described in detail in the earlier works. The MEM peaks highlighted in the figures are all peaks that are consistently present over a series of temperatures (and samples) and show systematic behavior consistent with not being an artifact. Some of the line shapes appear more narrow than anticipated especially for the weaker bands. This narrowing may be an artifact of over-fitting but the peak positions which are the focus in this study are essentially invariant with respect to the iterations needed to generate the populations with reasonable chi squares.

Figures 2 and 3 show the broad array of patterns associated with CO recombination kinetic traces from wild type (sperm whale) and mutant COMbs encapsulated in porous sol-matrices that are bathed in glycerol. We use the designation of 100% glycerol to indicate that the aqueous buffer initially covering the sol-gel sample has been replaced with a large excess of pure CO purged glycerol. It is possible that there is still a trace of water that remains trapped in the sol-gel under these conditions. The hygroscopic nature of glycerol makes it difficult to prepare glycerol bathed samples that are all identical with respect to residual water content. Since the glycerol/water ratio has been shown to have clear effect on the relative amplitudes and onset of the kinetic phases (Khan et al., 2000; Khan et al., 2001; Sottini et al., 2004; Sottini et al., 2005a; Sottini et al., 2005b; Sottini et al., 2005c), it is possible that anticipated small variations in water content in different glycerol bathed sol-gel samples may influence the time points for the onset of the C and D state dynamics. There are also clear indications that the templated environment surrounding the encapsulated protein differs from that of bulk solvent in the pores of sol-gel that link the interior to the exterior of the sol-gel (Massari et al., 2006). The solvent within the pores appears to have diffusion and viscosity properties similar to the bulk solvent whereas the reduced-volume hydration shell surrounding the encapsulated protein creates enhanced viscosity relative to the bulk. At this stage we do not know the extent to which the water and glycerol partition in the hydration layer of the encapsulated protein but there is the possibility of enhanced effects due to variations in trace amounts of water in samples bathed in “pure” glycerol. The vibrational echo measurements of Fayer and coworkers (Massari et al., 2005; Massari et al., 2006) should able to resolve this issue by providing the effective local viscosity modulating vibrational dephasing processes.

The shown range of patterns for CO recombination at high viscosity shown in Figures 2 and 3 contains kinetic traces that are representative of most if not all Mbs and Hbs that we have examined including those from truncated Hbs (Samuni et al., 2003; Dantsker et al., 2004). The mutant Mbs, all of which contain distal hemepocket substitutions, have been well characterized as described in the earlier studies (Dantsker et al., 2005a; Dantsker et al., 2005b). The H64L mutation replaces the E7 distal histidine with a leucine resulting in a DHP that is apolar and in loss of the steric and dynamic contributions of the large mobile imidazole side chain. The 64L side chain has been shown to be essentially neutral with respect to steric hindrance (Quillin et al., 1993) and in the H64L single mutant eliminates the entry of water into the DHP

subsequent to ligand photodissociation (Cao et al., 2001). The H64L series of double mutants in which the second mutation is at the residue 68(E11) site has been shown to be an effective series for exposing the role of the E11 side chain in modulating the CO recombination in the absence of the strong influence of the H64 side chain and of the H64 mediated entry of water into the vacated DHP (Dantsker et al., 2005a). The L29(B10)W mutation introduces a large mobile indole side chain at a site where it can both modulate ligand diffusion and contribute to significant enhancement of the barrier for recombination when it relaxes to a position above the heme iron subsequent to the CO vacating the DHP (Dantsker et al., 2002; Dantsker et al., 2005a).

The traces in Figures 2 and 3 are arranged in a progression to illustrate the concepts and nomenclature that are part of the presented model. This point is further emphasized by the arrows shown on the bottom of Fig. 2 that both signify the onset of the functional influence and duration of the different tiers of dynamics. Each dynamic state (arrow) is labeled with a designation for the category of motion to which that tier of dynamics is slaved. The segments of the traces bracketed by the designations: B→A, C→A and D→A designate the recombination occurring during the B, C and D state temporal windows. Consequently these brackets also show the temporal window over which the protein-ligand system is not being influenced by a given tier of dynamics. Thus the B→A bracket indicates the temporal window starting at the instant of photodissociation (time zero) during which neither the C or D tier of dynamics are operative. The C→A bracket shows the temporal window over which the C but not the D tier of dynamics is operative. The right edge end of the C→A bracket and the start of the D→A bracket signify the onset of the influence of the D tier of dynamics. The transitions between states (dynamic windows) are further indicated by arrows designated as B→C and C→D. These transition points are assigned based on breaks in the kinetic traces that occur at the same time point for a given temperature and solvent. Preliminary results that use the temperature dependence of the different breaks to calculate activation energies for the onset of the influence of the different tiers of dynamics yield numbers that are consistent with the slaving assignments shown above the arrows at the bottom of Fig. 2

The Figures show examples of traces that do not show the breaks because the recombination is essentially complete before the onset of either both transitions (e.g. H64L/V68F) or just the C→D transition (H64L/V68L at 3.5°C). Similarly if the recombination process within a given state is sufficiently slow, the signature of the dynamic transition is lost. This point is evident for the L29W mutant at 25° C (Fig 3) where the large indole side chain rapidly relaxes to a position that greatly slows the C→A phase so that the C→D transition is not apparent on the horizontal kinetic trace. It can also be seen in comparing Figures 2 and 3 that these transition times progress to earlier time points as the temperature increases from 3.5 to 25° C for these samples. The same temperature breaks in the traces are also seen for glycerol bathed encapsulated R and T state hemoglobins (unpublished results) prepared using the same protocol which is consistent with the idea these transitions are slaved to the solvent (Frauenfelder et al., 2002;Frauenfelder et al., 2006) but the consequences of the transitions are protein and mutant dependent.

The H64L/V68F mutant shows the fastest and least complicated recombination trace. The phenyl side chain at the 68(E11) site blocks access to the Xe cavities. The recombination traces shown for this mutant are assigned as the B→A phase. Figure 2 also shows the B→A phase for the H64L/V68A mutant. It can be seen that the kinetics are slower which has been attributed to the larger DHP volume associated with the A versus F substitution at the E11 site. The kinetic trace from H64L/V68L at 3.5° C, shown in Figure 2, illustrate how the B→A phase is terminated with the onset of the C dynamics which produce the C →A recombination phase. A comparison of the kinetics from this mutant at 3.5 and 25° C (Fig. 3) shows how at the higher temperature, the onset of the influence of the D tier of dynamics occurs at an early enough time

point to terminate the C →A phase and initiate the D→A phase. Wild type Mb shows all three phases at both temperatures. The recombination trace is consistent with the presence of the distal histidine both facilitating the escape of the CO from the DHP (under the influence of the C tier of dynamics) and through steric effects slowing the rebinding in the C state so that there is still a measurable population of unrecombined internal CO at the onset of the influence of the D tier dynamics (marked by the C→D arrow). Also included in Fig. 3 is the kinetic trace from H64L/V68N. A comparison of the traces from H64L/V68N, H64L/V68L, and wild type reveals that the for the former, the trace manifests a faster C→A phase and consequently, with the onset of the influence of the D state dynamics as indicated by the C→D arrow, the population having undergone C state recombination is larger for this protein than for the other two proteins, whereas for the wild type it is substantially lower.

9.1. The role of the E11 side chain

Figures 4–6 provide a comparison as a function of temperature of MEM generated kinetic populations in three different glycerol bathed sol-gel encapsulated H64L based double mutants. At the lowest temperature, all three mutants show the two components of the B→A phase. With increasing temperature, the slow B′→A phase is progressively lost. This loss is attributed to the progressively shorter onset time of the B→C transition which leads to an increase in the amplitude of the slower recombination due to the CO accessing a much larger internal volume. For the H64L/V68F mutant, the phenyl side chain decreases the probability of the CO escaping from the DHP into the adjacent Xe cavities and as a result the slower phase is not seen until much higher temperatures than for the other mutants. The much higher amplitude for the C population at all temperatures for the the H64L/V68L versus H64L/V68A mutants has been attributed to the requirement for adequate side chain motion to facilitate ligand diffusion. The large mobile side chain of the leucine is much more effective than the much shorter side chain of alanine. With increasing temperature the C state kinetic populations get faster and we start to see the emergence of the D state kinetic population reflecting the faster onset of the C→D transition. Mutant dependent differences in the rates of the D state recombination kinetics have been previously discussed in terms of hindered access to the iron based on the properties of the different E11 side chains (Dantsker et al., 2005a; Dantsker et al., 2005b). As noted earlier the D state recombination is under certain limits indistinguishable from the solvent phase bimolecular recombination. As long as one is in the limit of there being a high probability of a ligand within the protein matrix during the D state temporal window, there is no way to determine whether that ligand is the one that was initially dissociated or one that has entered from the solution during the D state temporal window.

9.2. Multiple C states

Figures 5 and 6 show that for the H64L/V68A and H64L/V68L mutants there is only distinguishable C state kinetic population. The slower recombination rates for these populations relative to the B state kinetic populations is attributed largely to the increase in accessible volume resulting from the C dynamics facilitating diffusion of the dissociated ligand. In Fig. 7 the MEM derived kinetic populations are shown for the single H64L mutant in a trehalose glass as a function of increasing exposure to humidity (a→c) which “loosens” the strong hydrogen bonding network comprising the glassy matrix (Cordone et al., 1998; Librizzi et al., 1999; Cottone et al., 2001; Cordone et al., 2005; Giuffrida et al., 2006). Under these conditions, the onset of the D state is sufficiently slow that no D state kinetic populations are observed (vide infra). In contrast to the samples that have either an alanine or leucine at the E11(68) site, the presence of the native valine at this site results in two C state populations (designated C and C′). This second slower population is attributed to a partial relaxation involving the E11 residue that brings the γ_2-methyl group of V68 closer to its fully relaxed equilibrium postion (for deoxy Mb) (Quillin et al., 1995; Dantsker et al., 2005a). The positioning of the γ_2-methyl group of the Val68 in the deoxy derivative, hinders access of the

ligand to the heme, thus increasing the barrier for CO bond formation. Fig. 7 also shows that with increasing exposure to moisture, the relative amplitude of the slower C′ kinetic population increases. This increase is consistent with a faster onset of the C→C′ transition giving rise to more of the dissociated population undergoing recombination under the influence of both the C and C′ "subtiers" of dynamics. Previously, it was shown that for a given high viscosity matrix, the relaxation accounting for the appearance of the C′ population has a higher activation energy than the dynamics giving rise to the first of the C state kinetic populations (Dantsker et al., 2005b).

9.3. The role of the distal histidine

Fig. 8 shows the kinetic traces and corresponding MEM derived kinetic populations for wild type COMb in a moderately dry glass as a function of temperature. Between −15 and 45°C, the recombination traces reflect the contribution of the B and C states. In this case there is a third member of the C state family which we label C″. This appearance of this population is tentatively attributed to the onset of a tier of C state dynamics that results in relaxation of the distal histidine to a position that further hinders ligand access to the heme. In the H64L mutants, this contribution is absent presumably due to the absence of the imidazole side chain. The kinetic trace in combination with the MEM shown in Fig. 8 illustrates how the three C state relaxation contribute to the lengthening and stretching of the overall C state recombination. Under low enough viscosity conditions, the onset of all three C substate tiers of dynamics is sufficiently fast that a single C state population experiencing the influence of all three subtiers of C dominates the kinetic pattern resulting in a more exponential process (as would be anticipated for a single C state population). The inset in Fig. 8 shows how when the temperature starts to approach the glass transition temperature (estimated to be near 70° C for this particular glass), the kinetic trace starts to show the break characteristic of the C→D transition that initiates the slower D state recombination. The MEM derived populations for the sample at 65° C shows the appearance of D state phases and the loss of the slowest C state phase. The loss of the slowest C state phase (C″) is readily accounted for by examining the corresponding kinetic trace and observing that the C→D transition is occurring on a comparable time scale as the C″ recombination. As a consequence, the D state dynamics take over and influence the overall recombination starting at that time point. Figure 9 shows how at a given temperature, the exposure of the glass to sufficient moisture (trace a) also results in the termination of the C state and the appearance of the D state recombination phase. The MEM suggests that under these conditions (trace a-moisture exposed), the three substates of the C manifold (C, C′, C″) may have coalesced into a single broad C state population.

9.4. Temperature dependence for the C→D transitions is solvent dependent

Figures 10a and 10b show the temperature dependence of the recombination traces and MEM derived kinetic populations for sol-gel encapsulated COMb bathed in glycerol. The MEM data show both how the different recombination phases become faster with increasing temperature and how different populations are lost as new ones appear as discussed earlier. The kinetic traces in Fig. 10a show the temporal progression for the C→D transition as a function of temperature. A comparison of the 25° C data from the glycerol bathed sample and the dry and wet glassy samples shows that the different matrices yield different patterns consistent with the concept that the protein dynamics are slaved to the solvent dynamics. The comparison between the pattern in the glycerol bathed gel and the dry glass clearly shows that the onset of the D state dynamics is very much later for the dry glass. The comparison between the wet glass and the glycerol bathed gel indicates that in the wet glass, the C tier of dynamics are operating on a faster time scale for the wet glass and yet the onset of the D state is still occurring at a later time point (~10^{-6} sec. versus ~ 2×10^{-5} seconds). The implication is that the volume changing D state protein dynamics suffer a proportionately greater degree of slow down when the solvent is comprised of a strong extended hydrogen bonded network of the kind that is

formed from concentrated sugar-water mixtures involving trehalose (Cottone et al., 2001; Cordone et al., 2005; Cottone et al., 2005). The strong extended hydrogen bonded network is expected to increase the energy penalty associated with the large degree of solvent reorganization needed to accommodate the volume changing dynamics of the protein.

In contrast to the C→D transition that is fully damped below the glass transition, consistent with the D state dynamics being slaved to the α fluctuations, the B→C transition still occurs in the glass over the range of temperatures used in this study. Sufficient drying of the glass does ultimately result in the full damping of the C state dynamics. These observations are consistent with other findings (Massari et al., 2005) supporting the concept that there are categories of motions such as the side chain fluctuations that are coupled to small amplitude motions (β fluctuations) of the hard to eliminate waters within the hydration shell of trehalose glasses (Cordone et al., 2005).

10. Conclusion

Protein dynamics can be organized in hierarchical groupings based on the degree to which each tier of dynamics is solvent slaved (Frauenfelder et al., 2001; Frauenfelder et al., 2002). For sufficiently high solvent viscosity, this ordering also produces an ordering with respect to the time window required for the onset of the influence of the dynamics. This temporal distinction among the different tiers is best observed at high viscosity conditions that allows for a clear separation of time scales based on the degree of solvent slaving. Photodissociation of ligands from hemeproteins and the subsequent rebinding over an extended time scale provides an excellent general system for exploring the sequential impact of the different tiers of dynamics. The advantage of this system is that the photodissociative event provides an initial time point (time zero) from which one can evaluate the onset of the influence of different dynamical events. Furthermore, the availability of different ligands, hemeproteins and mutant forms of hemeproteins provides the means to tune over an extensive range of time scales, the duration of the ligand recombination process thus providing a long enough functional process whose time course can provide signatures of the sequential onset of the different tiers of dynamics. The temperature dependence of these sets of time points for a given high viscosity solvent can be used to test solvent slaving concepts (Frauenfelder et al., 2006) and be used as an assay for the α and β solvent fluctuations for glassy materials. In the present work, the designations of B, C and D state are applied respectively to the protein plus dissociated ligand to indicate the temporal window during which the protein-ligand system is: i) not as yet experiencing the influence of the tiers of dynamics designated C and D, ii) experiencing the influence of the C tier of dynamics but not the D tier and iii) experiencing the influence of both tiers of dynamics. Thus from the instant of photodissociation, the recombination kinetics if long enough can exhibit the signatures of the sequential onset of influence for each tier of dynamics with the least solvent slaved tier (C state tier) manifesting its onset prior to the more strongly slaved tier (D). The concept applies to all proteins in that the probe time and solvent define which tiers of dynamics are impacting the measured process. The hemeprotein system is especially suitable for such studies in that there is a built in set point for a time zero at which instant the ligand is highly localized and the distribution of conformations well defined. This view can be extended to additional tiers of less and more highly slaved dynamics such as those associated with dynamic hole filling, full relaxation of the tertiary structure within myoglobins and relaxation of tertiary and quaternary structure in hemoglobins. In the sol-gel the tiers of dynamics associated with global tertiary and quaternary relaxation are sufficiently damped (with onset time of hours, days and weeks) that one can probe the B, C and D states as a function of the different equilibrium and non-equilibrium global tertiary and quaternary states.

Acknowledgements

This research was supported by National Institutes of Health Grant P01 HO071064.

References

Abadan Y, Chien EY, Chu K, Eng CD, Nienhaus GU, Sligar SG. Ligand binding to heme proteins. V. Light-induced relaxation in proximal mutants L89I and H97F of carbonmonoxymyoglobin. Biophys J 1995;68:2497–504. [PubMed: 7647252]

Abbruzzetti S, Giuffrida S, Sottini S, Viappiani C, Cordone L. Light-induced protein-matrix uncoupling and protein relaxation in dry samples of trehalose-coated MbCO at room temperature. Cell Biochem Biophys 2005;43:431–7. [PubMed: 16244367]

Abbruzzetti S, Viappiani C, Bruno S, Bettati S, Bonaccio M, Mozzarelli A. Functional characterization of heme proteins encapsulated in wet nanoporous silica gels. J Nanosci Nanotechnol 2001;1:407–15. [PubMed: 12914082]

Agmon N. Reactive line-shape narrowing in low-temperature inhomogeneous geminate recombination of CO to myoglobin. Biochemistry 1988;27:3507–11. [PubMed: 3390449]

Agmon N, Doster W, Post F. The transition from inhomogeneous to homogeneous kinetics in CO binding to myoglobin. Biophys J 1994;66:1612–22. [PubMed: 8061210]

Agmon N, Hopfield JJ. CO binding to heme proteins: A model for barrier height distributions and slow conformational changes. J Chem Phys 1983;79:2042–2053.

Ahmed AM, Campbell BF, Caruso D, Chance MR, Chavez MD, Courtney SH, Friedman JM, Iben IET, Ondrias MR, Yang M. Evidence for proximal control of ligand specificity in hemeproteins: absorption and Raman studies of cryogeneically trapped photoproducts of ligand bound myoglobins. Chem Phys 1991;158:329–351.

Alpert B, El Mohsni S, Lindqvist L, Tfibel F. Transient effects in the nanosecond laser photolysis of carbonmonoxyhemoglobin: Cage recombination and spectral evolution of the protein. Chem Phys Letters 1979;64:11–16.

Ansari A, Jones CM, Henry ER, Hofrichter J, Eaton WA. Conformational relaxation and ligand rebinding in myoglobin. Science 1992;256:1796–1798. [PubMed: 1615323]

Antonini, E.; Brunori, M. Hemoglobins and Myoglobins in their Reactions with Ligands. North-Holland Publishing Co.; Amsterdam: 1971.

Aranda, Rt; Levin, EJ.; Schotte, F.; Anfinrud, PA.; Phillips, GN, Jr. Time-dependent atomic coordinates for the dissociation of carbon monoxide from myoglobin. Acta Crystallogr D Biol Crystallogr 2006;62:776–83. [PubMed: 16790933]

Austin RH, Beeson K, Eisenstein L, Frauenfelder H, Gunsalus IC, Marshall VP. Dynamics of carbon monoxide binding by heme proteins. Science 1973;181:541–3. [PubMed: 4721048]

Austin RH, Beeson KW, Eisenstein L, Frauenfelder H, Gunsalus IC. Dynamics of ligand binding to myoglobin. Biochemistry 1975;14:5355–5373. [PubMed: 1191643]

Bettati S, Mozarrelli A. T State Binds Oxygen Noncooperatively with Allosteric Effects of Protons, IHP and Chloride. J Biol Chem 1997;272:32050–32055. [PubMed: 9405399]

Bourgeois D, Vallone B, Arcovito A, Sciara G, Schotte F, Anfinrud PA, Brunori M. Extended subnanosecond structural dynamics of myoglobin revealed by Laue crystallography. Proc Natl Acad Sci U S A 2006;103:4924–9. [PubMed: 16547137]

Bourgeois D, Vallone B, Schotte F, Arcovito A, Miele AE, Sciara G, Wulff M, Anfinrud P, Brunori M. Complex landscape of protein structural dynamics unveiled by nanosecond Laue crystallography. Proc Natl Acad Sci U S A 2003;100:8704–9. [PubMed: 12847289]

Bruno S, Bonaccio M, Bettati S, Rivetti C, Viappiani C, Abbruzzetti S, Mozzarelli A. High and low oxygen affinity conformations of T state hemoglobin. Protein Sci 2001;10:2401–7. [PubMed: 11604545]

Brunori M, Cutruzzola F, Savino C, Travaglini-Allocatelli C, Vallone B, Gibson QH. Structural dynamics of ligand diffusion in the protein matrix: A study on a new myoglobin mutant Y(B10) Q(E7) R(E10). Biophys J 1999;76:1259–69. [PubMed: 10049310]

Brunori M, Vallone B, Cutruzzola F, Travaglini-Allocatelli C, Berendzen J, Chu K, Sweet RM, Schlichting I. The role of cavities in protein dynamics: crystal structure of a photolytic intermediate of a mutant myoglobin. Proc Natl Acad Sci U S A 2000;97:2058–63. [PubMed: 10681426]

Campbell BF, Chance MR, Friedman JM. Linkage of functional and structural heterogeneity in proteins: dynamic hole burning in carboxymyoglobin. Science 1987;238:373–6. [PubMed: 3659921]

Cao W, Christian JF, Champion PM, Rosca F, Sage JT. Water penetration and binding to ferric myoglobin. Biochemistry 2001;40:5728–37. [PubMed: 11341838]

Chavez MD, Courtney SH, Chance MR, Kuila D, Nocek J, Hoffman BM, Friedman JM, Ondrias MR. Structural and functional significance of inhomogeneous line broadening of band III in hemoglobin and Fe-Mn hybrid hemoglobins. Biochemistry 1990;29:4844–4852. [PubMed: 2364063]

Cordone L, Cottone G, Giuffrida S, Palazzo G, Venturoli G, Viappiani C. Internal dynamics and protein-matrix coupling in trehalose-coated proteins. Biochim Biophys Acta 2005;1749:252–81. [PubMed: 15886079]

Cordone L, Galajda P, Vitrano E, Gassmann A, Ostermann A, Parak F. A reduction of protein specific motions in co-ligated myoglobin embedded in a trehalose glass. European Biophysics Journal with Biophysics Letters 1998;27:173–176. [PubMed: 10950639]

Cottone G, Cordone L, Ciccotti G. Molecular dynamics simulation of carboxy-myoglobin embedded in a trehalose-water matrix. Biophys J 2001;80:931–8. [PubMed: 11159460]

Cottone G, Giuffrida S, Ciccotti G, Cordone L. Molecular dynamics simulation of sucrose- and trehalose-coated carboxy-myoglobin. Proteins 2005;59:291–302. [PubMed: 15723350]

Dantsker D, Roche C, Samuni U, Blouin G, Olson JS, Friedman JM. The position 68(E11) side chain in myoglobin regulates ligand capture, bond formation with heme iron, and internal movement into the xenon cavities. J Biol Chem 2005a;280:38740–55. [PubMed: 16155005]

Dantsker D, Samuni U, Friedman AJ, Yang M, Ray A, Friedman JM. Geminate rebinding in trehalose-glass embedded myoglobins reveals residue-specific control of intramolecular trajectories. J Mol Biol 2002;315:239–251. [PubMed: 11779242]

Dantsker D, Samuni U, Friedman JM, Agmon N. A hierarchy of functionally important relaxations within myoglobin based on solvent effects, mutations and kinetic model. Biochim Biophys Acta 2005b; 1749:234–51. [PubMed: 15914102]

Dantsker D, Samuni U, Ouellet Y, Wittenberg BA, Wittenberg JB, Milani M, Bolognesi M, Guertin M, Friedman JM. Viscosity dependent relaxation significantly modulates the kinetics of CO recombination in the truncated hemoglobin trHbN from mycobacterium tuberculosis. J Biol Chem. 2004

Das TK, Khan I, Rousseau DL, Friedman JM. Temperature dependent quaternary state relaxation in sol-gel encapsulated hemoglobin. Biospectroscopy 1999;5:S64–70. [PubMed: 10512539]

Doster, W.; Kleinert, T.; Post, F.; Settles, M. Effect of solvent on protein internal dynamics: The kinetics of ligand binding to myoglobin. In: Gregory, RB., editor. Protein-Solvent Interactions. Marcel Dekker; 1993. p. 375

Draghi F, Miele AE, Travaglini-Allocatelli C, Vallone B, Brunori M, Gibson QH, Olson JS. Controlling ligand binding in myoglobin by mutagenesis. J Biol Chem 2002;277:7509–19. [PubMed: 11744723]

Duddell DA, Morris RJ, Richards JT. Ultrafast Recombination in Nanosecond Laser Photolysis of Carbonylhemoglobin. J Chem Soc Chem Commun 1979;2:75–76.

Fenimore PW, Frauenfelder H, McMahon BH, Parak FG. Slaving: solvent fluctuations dominate protein dynamics and functions. Proc Natl Acad Sci U S A 2002;99:16047–51. [PubMed: 12444262]

Frauenfelder H. Complexity in proteins. Nat Struct Biol 1995;2:821–3. [PubMed: 7552700]

Frauenfelder H, Fenimore PW, Chen G, McMahon BH. Protein folding is slaved to solvent motions. Proc Natl Acad Sci U S A 2006;103:15469–72. [PubMed: 17030792]

Frauenfelder H, Fenimore PW, McMahon BH. Hydration, slaving and protein function. Biophys Chem 2002;98:35–48. [PubMed: 12128188]

Frauenfelder H, McMahon BH, Austin RH, Chu K, Groves JT. The role of structure, energy landscape, dynamics, and allostery in the enzymatic function of myoglobin. Proc Natl Acad Sci U S A 2001;98:2370–2374. [PubMed: 11226246]

Frauenfelder H, Sligar SG, Wolynes PG. The energy landscapes and motions of proteins. Science 1991;254:1598–603. [PubMed: 1749933]

Friedman JM, Lyons KB. Transient Raman study of CO-haemoprotein photolysis: origin of the quantum yield. Nature 1980;284:570–572. [PubMed: 7366727]

Giuffrida S, Cottone G, Cordone L. Role of solvent on protein-matrix coupling in MbCO embedded in water-saccharide systems: a Fourier transform infrared spectroscopy study. Biophys J 2006;91:968–80. [PubMed: 16714349]

Hagen SJ, Hofrichter J, Eaton WA. Geminate Rebinding and Conformational Dynamics of Myoglobin Embedded in a Glass at Room Temperature. Journal of Physical Chemistry 1996;100:12008–12021.

Hartmann H, Zinser S, Komninos P, Schneider RT, Nienhaus GU, Parak F. X-ray structure determination of a metastable state of carbonmonoxy myoglobin after photodissociation. Proc Natl Acad Sci U S A 1996;93:7013–6. [PubMed: 8692935]

Henry ER, Sommer JH, Hofrichter J, Eaton WA. Geminate Recombination of Carbon Monoxide to Myoglobin. J Mol Biol 1983;166:443–451. [PubMed: 6854651]

Huang J, Ridsdale A, Wang J, Friedman JM. Kinetic Hole Burning, Hole Filling, and Conformational Relaxation in Heme Proteins: Direct Evidence for the Functional Significance of a Hierarchy of Dynamical Processes. Biochemistry 1997;36:14353–14365. [PubMed: 9398153]

Hummer G, Schotte F, Anfinrud PA. Unveiling functional protein motions with picosecond x-ray crystallography and molecular dynamics simulations. Proc Natl Acad Sci U S A 2004;101:15330–4. [PubMed: 15489270]

Khan I, Dantsker D, Samuni U, Friedman AJ, Bonaventura C, Manjula B, Acharya SA, Friedman JM. Beta 93 modified hemoglobin: kinetic and conformational consequences. Biochemistry 2001;40:7581–92. [PubMed: 11412112]

Khan I, Shannon CF, Dantsker D, Friedman AJ, Perez-Gonzalez-de-Apodaca J, Friedman JM. Sol-gel trapping of functional intermediates of hemoglobin: geminate and bimolecular recombination studies. Biochemistry 2000;39:16099–109. [PubMed: 11123938]

Kleinert T, Doster W, Leyser H, Petry W, Schwarz V, Settles M. Solvent composition and viscosity effects on the kinetics of CO binding to horse myoglobin. Biochemistry 1998;37:717–733. [PubMed: 9425096]

Kriegl JM, Nienhaus K, Deng P, Fuchs J, Nienhaus GU. Ligand dynamics in a protein internal cavity. Proc Natl Acad Sci U S A 2003;100:7069–74. [PubMed: 12773621]

Lamb DC, Arcovito A, Nienhaus K, Minkow O, Draghi F, Brunori M, Nienhaus GU. Structural dynamics of myoglobin: an infrared kinetic study of ligand migration in mutants YQR and YQRF. Biophys Chem 2004;109:41–58. [PubMed: 15059658]

Librizzi F, Viappiani C, Abbruzzetti S, Cordone L. Resual water modulates the dynamics of the protein and of the external matrix in trehalose coated MbCO. J Chem Phys 2002;116:1193–1200.

Librizzi F, Vitrano E, Cordone L. Dehydration and crystallization of trehalose and sucrose glasses containing carbonmonoxy-myoglobin. Biophys J 1999;76:2727–34. [PubMed: 10233087]

Lim M, Anfinrud PA. Ultrafast time-resolved IR studies of protein-ligand interactions. Methods Mol Biol 2005;305:243–60. [PubMed: 15940001]

Lim M, Jackson TA, Anfinrud PA. Orientational distribution of CO before and after photolysis of MbCO and HbCO: a determination using time-resolved polarized Mid-IR spectroscopy. J Am Chem Soc 2004;126:7946–57. [PubMed: 15212544]

Lubchenko V, Wolynes PG, Frauenfelder H. Mosaic energy landscapes of liquids and the control of protein conformational dynamics by glass-forming solvents. J Phys Chem B Condens Matter Mater Surf Interfaces Biophys 2005;109:7488–99. [PubMed: 16851860]

Massari AM, Finkelstein IJ, Fayer MD. Dynamics of proteins encapsulated in silica sol-gel glasses studied with IR vibrational echo spectroscopy. J Am Chem Soc 2006;128:3990–7. [PubMed: 16551107]

Massari AM, Finkelstein IJ, McClain BL, Goj A, Wen X, Bren KL, Loring RF, Fayer MD. The influence of aqueous versus glassy solvents on protein dynamics: vibrational echo experiments and molecular dynamics simulations. J Am Chem Soc 2005;127:14279–89. [PubMed: 16218622]

Nienhaus GU, Mourant JR, Frauenfelder H. Spectroscopic evidence for conformational relaxation in myoglobin. Proc Natl Acad Sci U S A 1992;89:2902–6. [PubMed: 1557397]

Nienhaus K, Deng P, Kriegl JM, Nienhaus GU. Structural dynamics of myoglobin: effect of internal cavities on ligand migration and binding. Biochemistry 2003a;42:9647–58. [PubMed: 12911306]

Nienhaus K, Deng P, Kriegl JM, Nienhaus GU. Structural dynamics of myoglobin: spectroscopic and structural characterization of ligand docking sites in myoglobin mutant L29W. Biochemistry 2003b; 42:9633–46. [PubMed: 12911305]

Olson JS, Phillips GN. Kinetic pathways and barriers for ligand binding to myoglobin. J Biol Chem 1996;271:17593–17596. [PubMed: 8698688]

Ostermann A, Waschipky R, Parak FG, Nienhaus GU. Ligand binding and conformational motions in myoglobin. Nature 2000;404:205–8. [PubMed: 10724176]

Powers L, Chance B, Chance M, Campbell B, Friedman J, Khalid S, Kumar C, Naqui A, Reddy KS, Zhou Y. Kinetic, structural, and spectroscopic identification of geminate states of myoglobin: a ligand binding site on the reaction pathway. Biochemistry 1987;26:4785–96. [PubMed: 3663626]

Quillin ML, Arduini RM, Olson JS, Phillips GN. High-resolution crystal structures of distal histidine mutants of sperm shale myoglobin. J Mol Biol 1993;234:140–155. [PubMed: 8230194]

Quillin ML, Li T, Olson JS, Phillips GN Jr, Dou Y, Ikeda-Saito M, Regan R, Carlson M, Gibson QH, Li H, et al. Structural and functional effects of apolar mutations of the distal valine in myoglobin. J Mol Biol 1995;245:416–36. [PubMed: 7837273]

Samuni U, Dantsker D, Juszczak LJ, Bettati S, Ronda L, Mozzarelli A, Friedman JM. Spectroscopic and functional characterization of T state hemoglobin conformations encapsulated in silica gels. Biochemistry 2004;43:13674–82. [PubMed: 15504030]

Samuni U, Dantsker D, Khan I, Friedman AJ, Peterson E, Friedman JM. Spectroscopically and kinetically distinct conformational populations of sol-gel-encapsulated carbonmonoxy myoglobin. A comparison with hemoglobin. J Biol Chem 2002;277:25783–90. [PubMed: 11976324]

Samuni U, Dantsker D, Ray A, Wittenberg JB, Wittenberg BA, Dewilde S, Moens L, Ouellet Y, Guertin M, Friedman JM. Kinetic modulation in carbonmonoxy derivatives of truncated hemoglobins: the role of distal heme pocket residues and extended apolar tunnel. J Biol Chem 2003;278:27241–50. [PubMed: 12736253]

Samuni U, Roche CJ, Dantsker D, Juszczak LJ, Friedman JM. Modulation of reactivity and conformation within the T-quaternary state of human hemoglobin: the combined use of mutagenesis and sol-gel encapsulation. Biochemistry 2006;45:2820–35. [PubMed: 16503637]

Schoenborn BP, Watson HC, Kendrew JC. Binding of xenon to sperm whale myoglobin. Nature 1965;207:28–30. [PubMed: 5893727]

Schotte F, Lim M, Jackson TA, Smirnov AV, Soman J, Olson JS, Phillips GN Jr, Wulff M, Anfinrud PA. Watching a protein as it functions with 150-ps time-resolved x-ray crystallography. Science 2003;300:1944–7. [PubMed: 12817148]

Schotte F, Soman J, Olson JS, Wulff M, Anfinrud PA. Picosecond time-resolved X-ray crystallography: probing protein function in real time. J Struct Biol 2004;147:235–46. [PubMed: 15450293]

Scott EE, Gibson QH. Ligand migration in sperm whale myoglobin. Biochemistry 1997;36:11909–17. [PubMed: 9305984]

Scott EE, Gibson QH, Olson JS. Mapping the pathways for O2 entry into and exit from myoglobin. J Biol Chem 2000;3:3.

Scott EE, Gibson QH, Olson JS. Mapping the pathways for O2 entry into and exit from myoglobin. J Biol Chem 2001;3:3.

Shibayama N, Saigo S. Oxygen equilibrium properties of myoglobin locked in the liganded and unliganded conformations. J Am Chem Soc 2003;125:3780–3. [PubMed: 12656610]

Sottini S, Abbruzzetti S, Spyrakis F, Bettati S, Ronda L, Mozzarelli A, Viappiani C. Geminate rebinding in R-state hemoglobin: kinetic and computational evidence for multiple hydrophobic pockets. J Am Chem Soc 2005a;127:17427–32. [PubMed: 16332093]

Sottini S, Abbruzzetti S, Viappiani C, Bettati S, Ronda L, Mozzarelli A. Evidence for two geminate rebinding states following laser photolysis of R state hemoglobin encapsulated in wet silica gels. J Phys Chem B Condens Matter Mater Surf Interfaces Biophys 2005b;109:11411–3. [PubMed: 16852394]

Sottini S, Abbruzzetti S, Viappiani C, Ronda L, Mozzarelli A. Determination of microscopic rate constants for CO binding and migration in myoglobin encapsulated in silica gels. J Phys Chem B Condens Matter Mater Surf Interfaces Biophys 2005c;109:19523–8. [PubMed: 16853522]

Sottini S, Viappiani C, Ronda L, Bettati S, Mozzarelli A. CO Rebinding Kinetics to Myoglobin- and R-State-Hemoglobin-Doped Silica Gels in the Presence of Glycerol. J Phys Chem B 2004;108:8475–8484.

Srajer V, Champion PM. Investigations of optical line shapes and kinetic hole burning in myoglobin. Biochemistry 1991;30:7390–402. [PubMed: 1854744]

Srajer V, Reinisch L, Champion PM. Investigation of laser-induced long-lived states of photolyzed MbCO. Biochemistry 1991;30:4886–95. [PubMed: 2036357]

Srajer V, Ren Z, Teng TY, Schmidt M, Ursby T, Bourgeois D, Pradervand C, Schildkamp W, Wulff M, Moffat K. Protein conformational relaxation and ligand migration in myoglobin: a nanosecond to millisecond molecular movie from time-resolved Laue X-ray diffraction. Biochemistry 2001;40:13802–15. [PubMed: 11705369]

Steinbach PJ, Ansari A, Berendzen J, Braunstein D, Chu K, Cowen BR, Ehrenstein D, Frauenfelder H, Johnson JB, Lamb DC, et al. Ligand binding to heme proteins: connection between dynamics and function. Biochemistry 1991;30:3988–4001. [PubMed: 2018767]

Teeter MM. Myoglobin cavities provide interior ligand pathway. Protein Sci 2004;13:313–8. [PubMed: 14739317]

Tetreau C, Blouquit Y, Novikov E, Quiniou E, Lavalette D. Competition with xenon elicits ligand migration and escape pathways in myoglobin. Biophys J 2004;86:435–47. [PubMed: 14695286]

Tilton RF, Kuntz ID, Petsko GA. Cavities in proteins: Structure of a Metmyoglobin-Xenon complex solved to 1.9 Å resolution. Biochemistry 1984;23:2849–2857. [PubMed: 6466620]

Viappiani C, Bettati S, Bruno S, Ronda L, Abbruzzetti S, Mozzarelli A, Eaton WA. New insights into allosteric mechanisms from trapping unstable protein conformations in silica gels. Proc Natl Acad Sci U S A 2004;101:14414–9. [PubMed: 15385676]

Wullf M, Plech A, Eybert L, Randler R, Schotte F, Anfinrud P. The realization of sub-nanosecond pump and probe experiments at the ESRF. European Synchrotron Radiation Facility. Faraday Discuss 2003;122:13–26. 79–88. [PubMed: 12555847]

Abbreviations

DHP
: distal heme pocket

HAM
: heme access modes

KHB
: kinetic hole burning

Mb
: myoglobin

MEM
: maximum entropy method

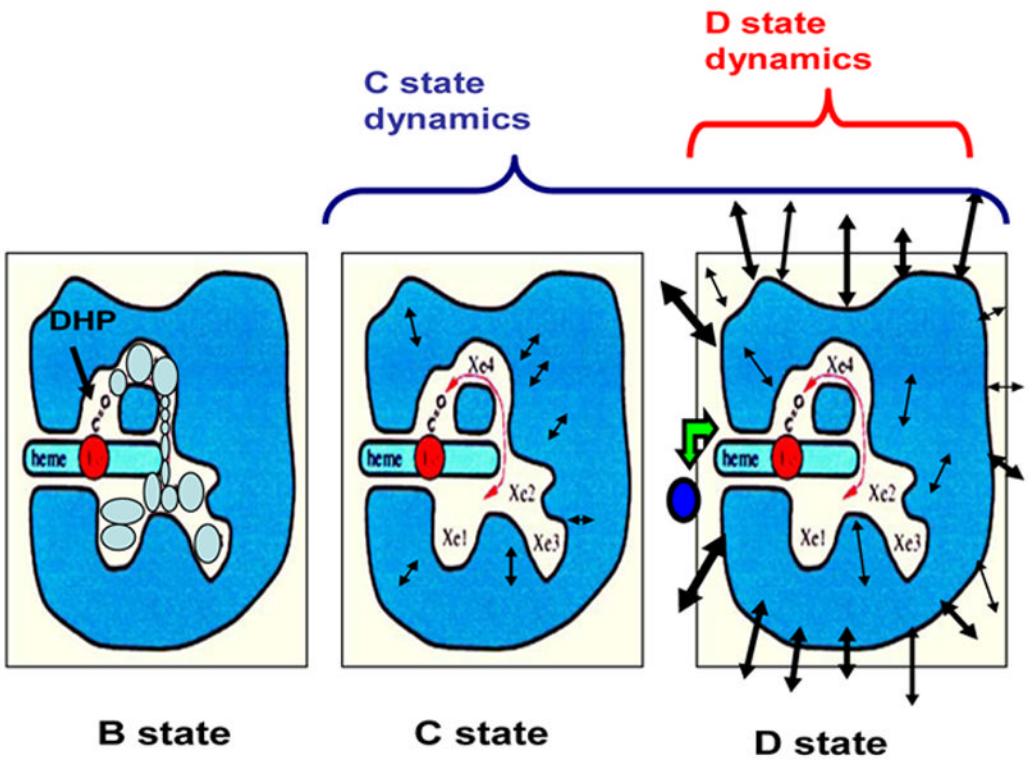

Figure 1.
A schematic illustrating the concept that for COMb photodissociated at time zero, there is a progression of different "states" defined by which tier of solvent slaved dynamics is operative. During the first time window (starting at time zero), the two solvent slaved tiers of dynamics (C and D state dynamics) are not as yet influencing the properties of the photoproduct. The photoproduct population during this first time window is designated as being in the B state. With the sequential onset of influence of the C and D state dynamics, the population evolves into the C and D states respectively. Under the influence of the C state dynamics, there is side chain facilitated diffusion of the ligand within the protein (Xe cavities and distal heme pocket) but no exchange of ligand or solvent molecules with the surrounding solvent/matrix. Under the influence of the larger amplitude D state dynamic, there is potential exchange of water molecules and ligands between protein and solvent.

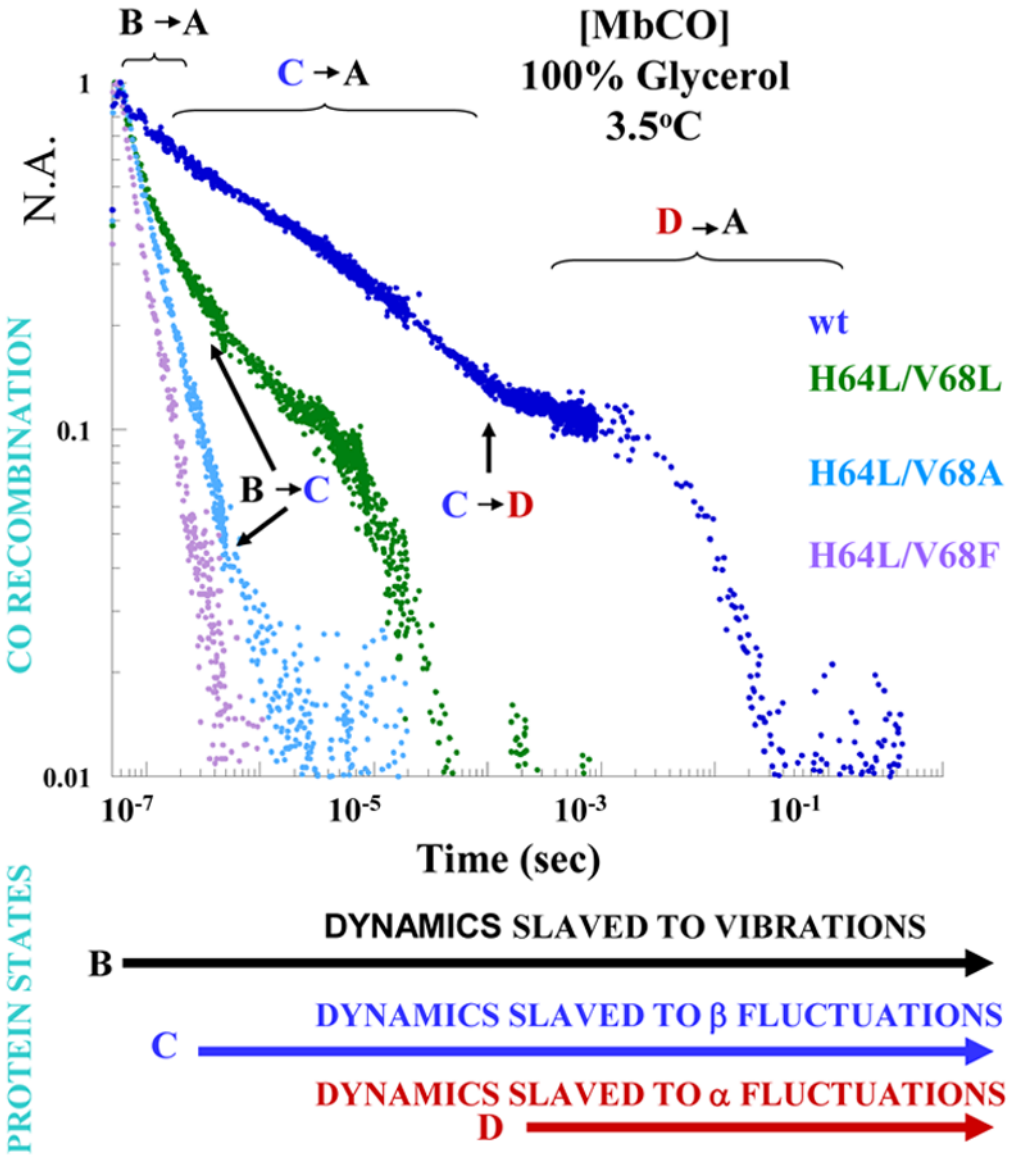

Figure 2.

The 3.5° C CO recombination traces for wild type and double mutant myoglobins encapsulated in porous sol-gel matrices (designated by the brackets) bathed in glycerol. The recombination traces are displayed on a log log plot of normalized absorbance (NA) at 442 nm versus time subsequent to photodissociation using 7 ns 532 nm pulses at 2 Hz. The traces are arranged to show the range the range of kinetic patterns. The B→A, C→A and D →A labels show the recombination phase associated with the B, C and D states. The B→C and C→D arrows show the very approximate time point for the onset of the influence of the C and D state tier of dynamics respectively.

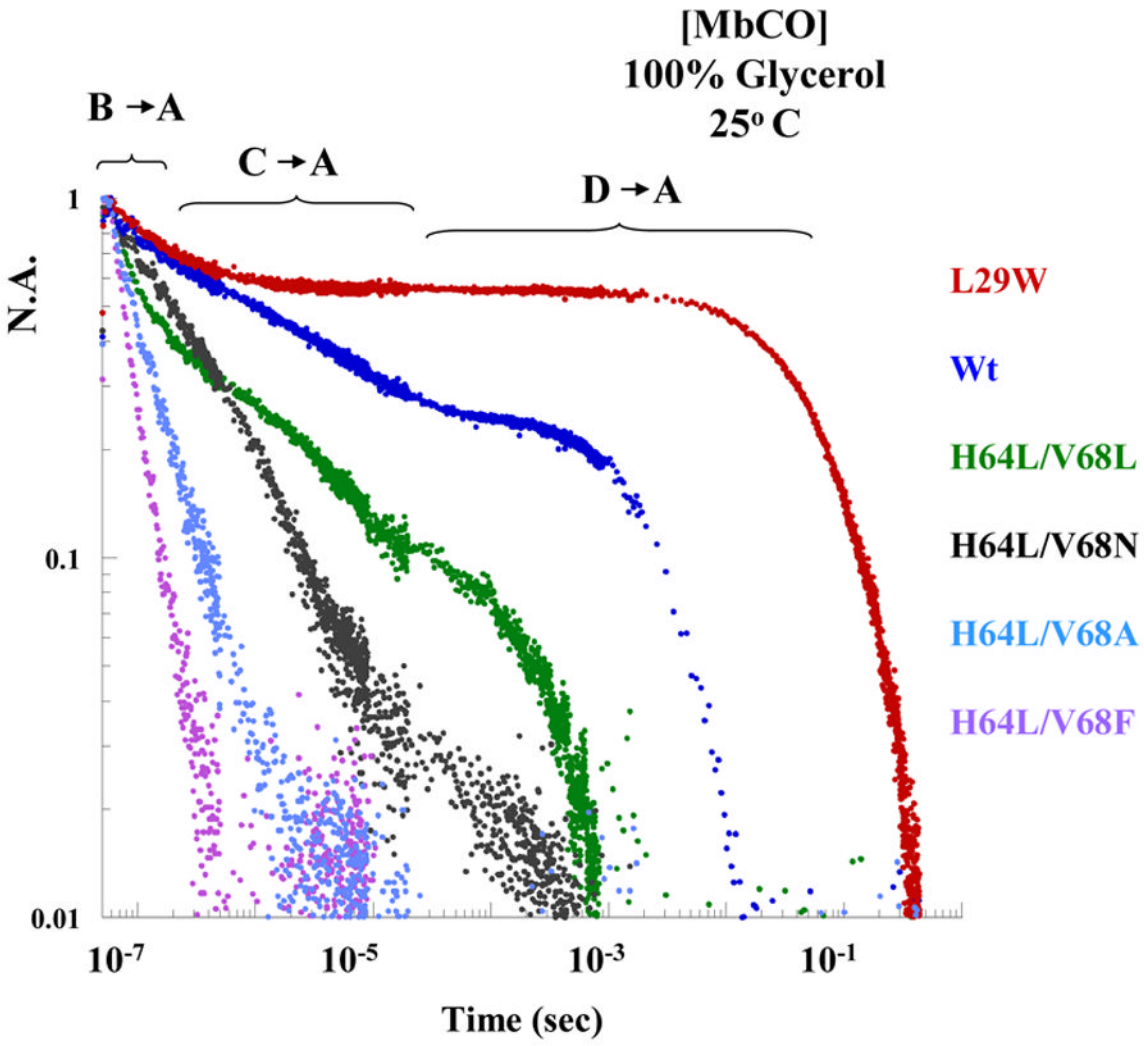

Figure 3.

The 25°C CO recombination traces for wild type and mutant myoglobins encapsulated in porous sol-gel matrices and bathed in glycerol. Note that the C→D transition for the different mutants is at the same time point but the consequences with respect to recombination are protein dependent. The absence of a C→A phase for Mb(L29W) precludes seeing the seeing the signature of the C→D transition in the recombination trace. Similarly the fast completion of the recombination process for the Mb(H64L/V68F) mutant also precludes seeing any of the transitions that are occurring on slower time scale.

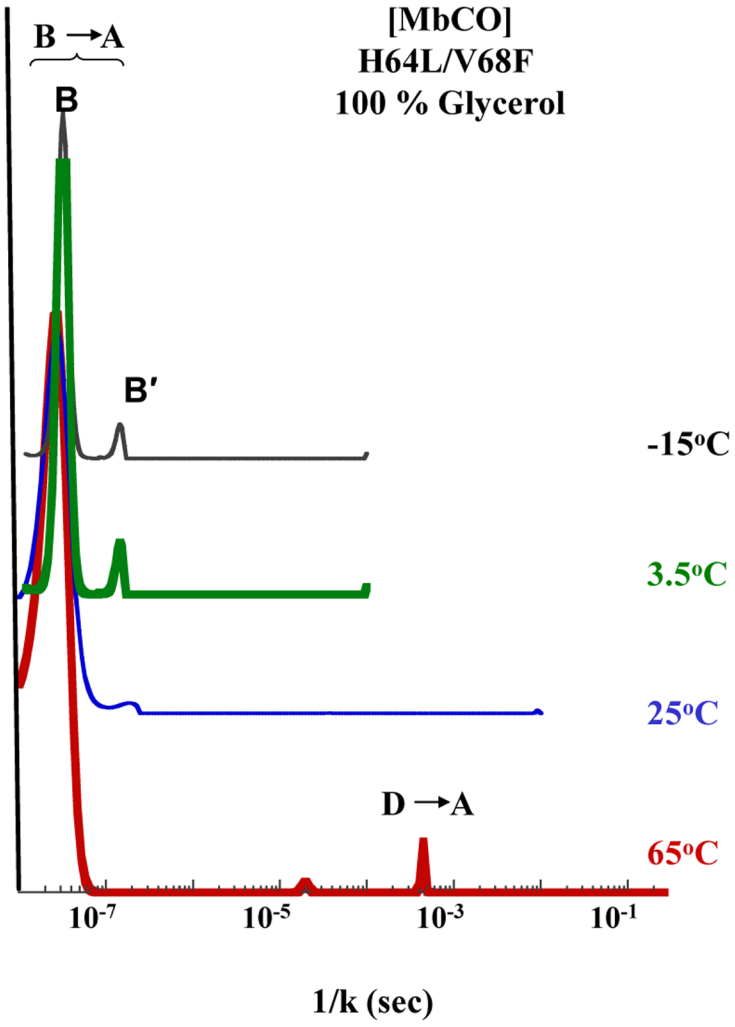

Figure 4.

The temperature dependence of MEM kinetic populations derived from the CO recombination traces from sol-gel encapsulated Mb(H64L/V68F) bathed in glycerol. The Y axis represents the amplitude for relative population. The peaks represent population having recombination time constants (k) that are the reciprocal of the time points on the x axis where they occur.

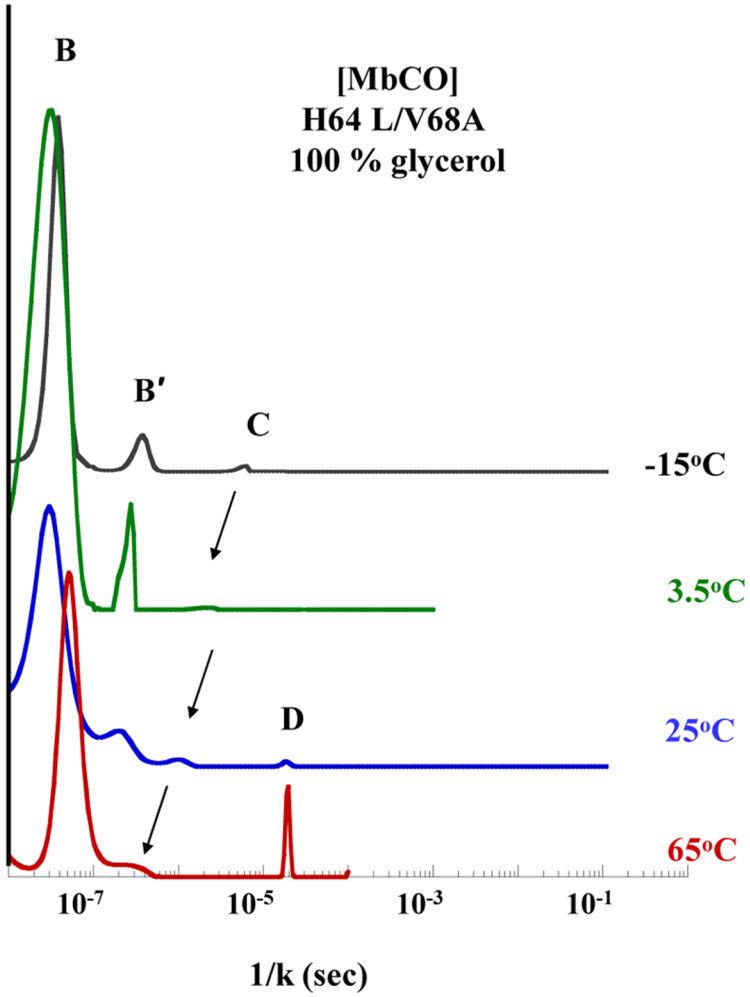

Figure 5.

The temperature dependence of MEM kinetic populations derived from the CO recombination traces from sol-gel encapsulated Mb(H64L/V68A) bathed in glycerol. The Y axis represents the amplitude for relative population. The peaks represent population having recombination time constants (k) that are the reciprocal of the time points on the x axis where they occur. The B, B′ labels refer to the populations associated with the two recombination phases of the B state whereas the C and D designations refer to the kinetic population derived from the C and D state respectively.

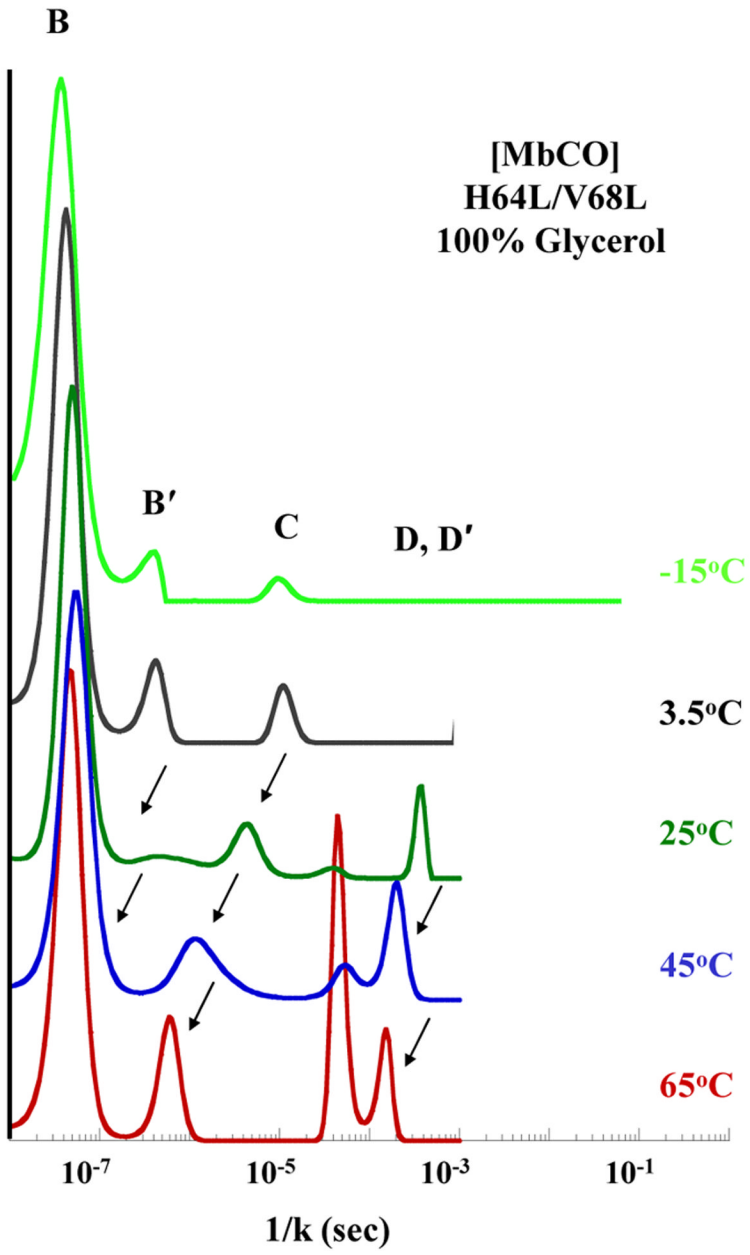

Figure 6.

The temperature dependence of MEM kinetic populations derived from the CO recombination traces from sol-gel encapsulated Mb(H64L/V68L) bathed in glycerol. See Figure 5 caption for details of nomenclature. The two D populations (D and D′) have been attributed to two different orientations of the 68L side chain. With decreasing viscosity of the solvent, the two populations are observed to coalesce into a single peak.

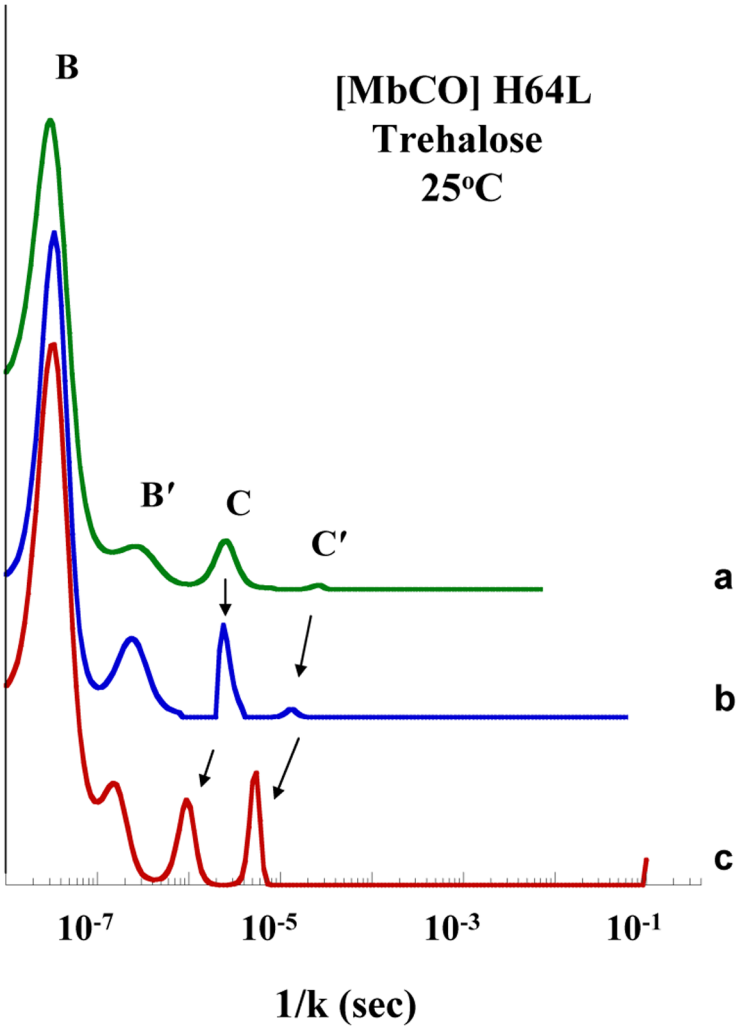

Figure 7.
The MEM kinetic populations at 25° C derived from the CO recombination traces from COMb (H64L) embedded in a trehalose glass. The sequence in going from trace *a* to trace *c* are the populations for the same glassy sample as a function of exposure time (several minutes) to a humid environment with sample *a* being the driest and sample *c* being the most exposed (the sample remained glassy through out the sequence). See Figure 5 caption for details of nomenclature. Note that in contrast to the two previous cases shown in Figures 5 and 6, there are now two C state kinetic populations (C and C′).

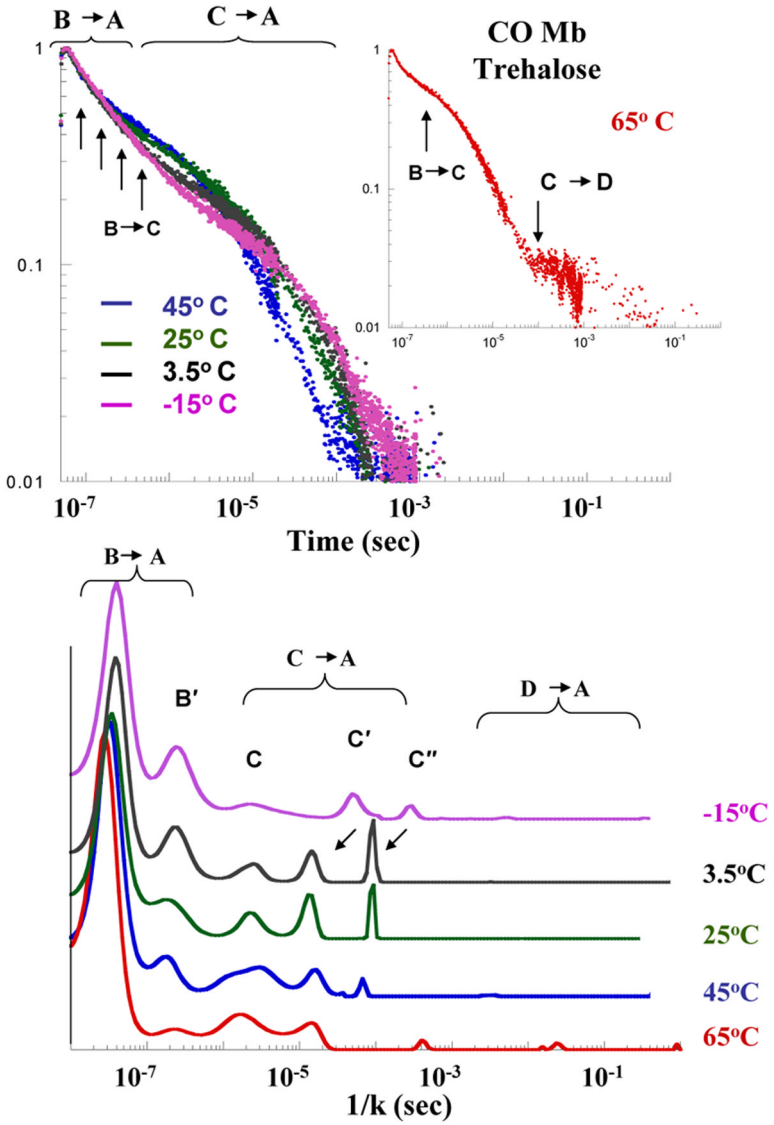

Figure 8.

Temperature dependence for CO recombination traces and corresponding MEM populations for wild type COMb embedded in a moderately dry trehalose glass matrix. Note that three C state populations (C, C′ and C″) are observable in contrast to two for Mb(H64L) and one for all of the H64L/V68X mutants (X = F, A, L, N).

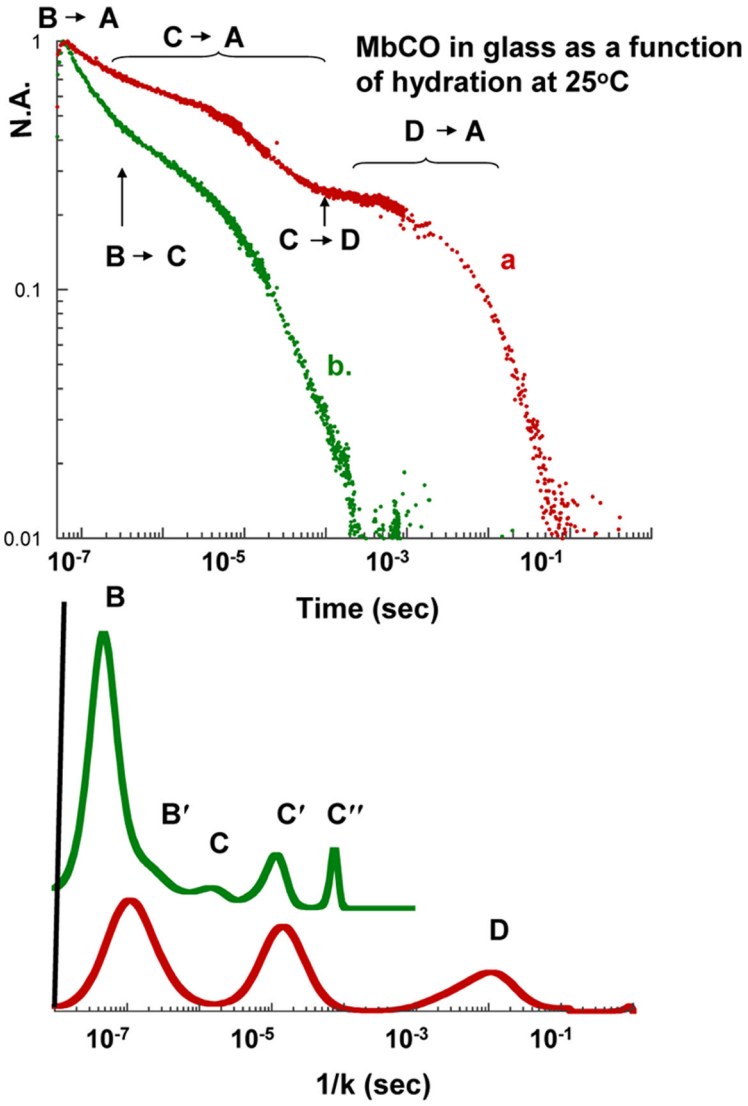

Figure 9.
CO recombination traces and MEM populations for COMb at 25° C in a trehalose glass before and after extended exposure to a humid atmosphere.

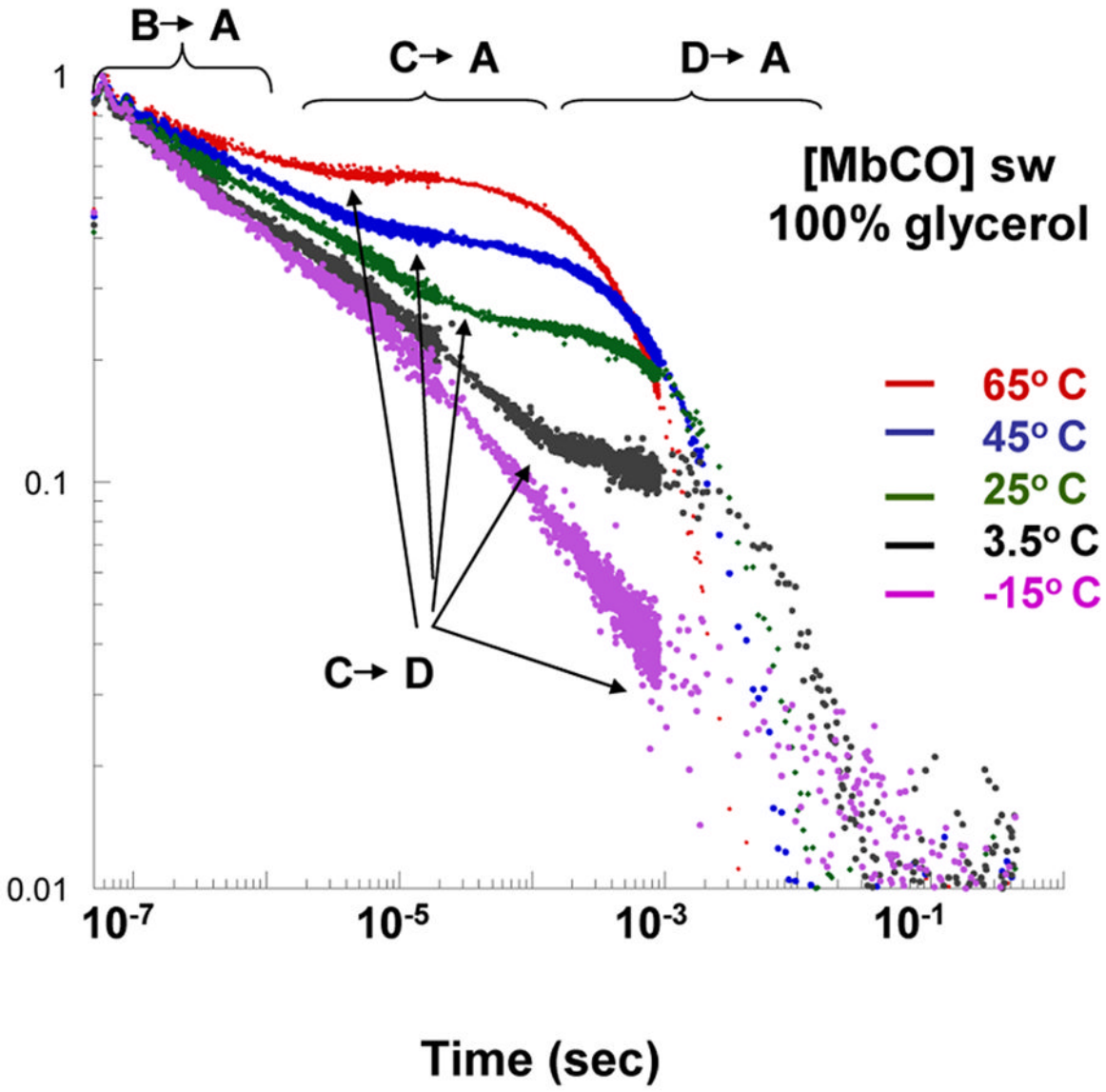

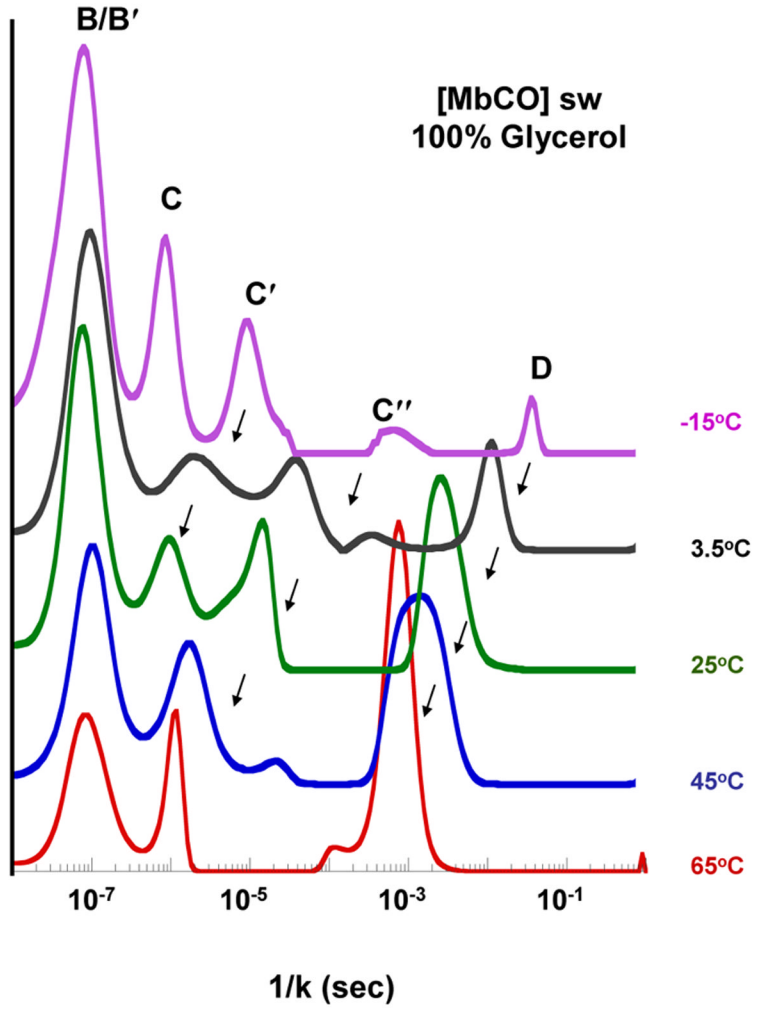

Figure 10.

The temperature dependence of the CO recombination traces (10a) and the MEM populations (10b) for sol-gel encapsulated COMb bathed in glycerol. In Fig 10a, the arrows expose the temperature dependence of the onset of the D state dynamics (C→D). The MEM population show how the different populations appear, disappear and evolve with temperature.